

# Exploiting Hierarchy for Learning and Transfer in KL-regularized RL

Dhruva Tirumala<sup>\*1</sup> Hyeonwoo Noh<sup>\*2</sup> Alexandre Galashov<sup>1</sup> Leonard Hasenclever<sup>1</sup> Arun Ahuja<sup>1</sup>  
 Greg Wayne<sup>1</sup> Razvan Pascanu<sup>1</sup> Yee Whye Teh<sup>1</sup> Nicolas Heess<sup>1</sup>

## Abstract

As reinforcement learning agents are tasked with solving more challenging and diverse tasks, the ability to incorporate prior knowledge into the learning system and to exploit reusable structure in solution space is likely to become increasingly important. The KL-regularized expected reward objective constitutes one possible tool to this end. It introduces an additional component, a default or prior behavior, which can be learned alongside the policy and as such partially transforms the reinforcement learning problem into one of behavior modelling. In this work we consider the implications of this framework in cases where both the policy and default behavior are augmented with latent variables. We discuss how the resulting hierarchical structures can be used to implement different inductive biases and how their modularity can benefit transfer. Empirically we find that they can lead to faster learning and transfer on a range of continuous control tasks.

## 1. Introduction

Reinforcement learning approaches, coupled with neural networks as function approximators, have solved an impressive range of tasks, from complex control tasks (Lillicrap et al., 2016; Heess et al., 2017; Riedmiller et al., 2018; Levine et al., 2016; OpenAI et al., 2018) to computer games (Mnih et al., 2015; OpenAI, 2018) and Go (Silver et al., 2016). Recent advances have greatly improved data efficiency, scalability, and stability of these algorithms in a variety of domains (Rennie et al., 2017; Zoph & Le, 2017; Espeholt et al., 2018; Ganin et al., 2018; Zhu et al., 2018).

Nevertheless, many tasks remain challenging to solve and require large numbers of interactions with the environment. While the reasons can be hard to pin down they frequently

have to do with the fact that solutions are unlikely to be found by chance when no prior knowledge is available, that the solution space is dominated by local optima, or that properties of the desired behaviour are not captured by the reward (e.g. natural movement of the body). Curricula, task distributions, demonstrations, among other approaches, have been shown to be powerful tools to overcome some of these problems. All these ideas rely critically on the ability to transfer behaviours across tasks, and thus on mechanisms for extracting knowledge about the structure of existing solutions from and for injecting prior knowledge into a reinforcement learning problem.

Probabilistic models are widely used across the machine learning community. They provide a rich set of tools to specify inductive biases, extract structure from data, to impose structure on learned solutions, as well as rules for composing model components. The KL-regularized objective (Todorov, 2007; Kappen et al., 2012; Rawlik et al., 2012; Schulman et al., 2017a) creates a connection between RL and probabilistic models. It introduces a second component, a prior or default behaviour, and the policy is then encouraged to remain close to it in terms of the Kullback-Leibler (KL) divergence – which can be used to influence the learned policy. Recently, within this framework, (Teh et al., 2017; Czarnecki et al., 2018; Goyal et al., 2019; Galashov et al., 2019) have proposed to learn a parametrized *default policy* in the role of a more informative prior.

These works suggest an elegant solution for enforcing complex biases that can be also learned or transferred from different tasks. And the objective provides much flexibility in terms of model and algorithm choice. However, its potential and limitations, and how to use it most effectively have not yet been studied well. It has been argued, e.g. (Galashov et al., 2019), that information asymmetry between the default policy and agent policy can be an efficient mechanism for discovering meaningful priors. Restricting the priors access to certain information (e.g. about the task) forces it to learn the expected behaviour that arises from marginalizing away this information, and the result can be understood as habitual behaviour of the agent.

In this work we extend this line of thought, considering the scenario when both the default policy and the agent are hier-

<sup>\*</sup>Equal contribution <sup>1</sup>DeepMind, London, UK <sup>2</sup>Department of Computer Science and Engineering, POSTECH, Pohang, Korea. Correspondence to: Dhruva Tirumala <dhruvat@google.com>, Hyeonwoo Noh <shgusdngogo@postech.ac.kr>.

archically structured and augmented with latent variables. This provides new mechanisms for restricting the information flow and introducing inductive biases. We present a general algorithmic framework in Appendix A, with the hierarchically structured variant elaborated in the main text and studied experimentally. In addition, we also explore how the resulting modular policies can be used in transfer learning scenarios. We provide empirical results on several tasks with physically simulated bodies and continuous action spaces as well as on discrete action grid worlds, highlighting the role of the structured policies.

## 2. RL as probabilistic modelling

In this section, we will provide an overview of how the KL-regularized objective can connect RL and probabilistic model learning, before developing our approach in the next section. We start by introducing some standard notation. We will denote states and actions at time  $t$  respectively with  $s_t$  and  $a_t$ .  $r(s, a)$  is the instantaneous reward received in state  $s$  when taking action  $a$ . We will refer to the history up to time  $t$  as  $x_t = (s_1, a_1, \dots, s_t)$  and the whole trajectory as  $\tau = (s_1, a_1, s_2, a_2, \dots)$ . The agent policy  $\pi(a_t|x_t)$  denotes a distribution over next actions given history  $x_t$ , while  $\pi_0(a_t|x_t)$  denotes a default or habitual policy.<sup>1</sup> The KL-regularized RL objective (Todorov, 2007; Kappen et al., 2012; Rawlik et al., 2012; Schulman et al., 2017a) takes the form:

$$\mathcal{L}(\pi, \pi_0) = \mathbb{E}_\tau \left[ \sum_{t \geq 1} \gamma^t r(s_t, a_t) - \alpha \gamma^t \text{KL}(a_t|x_t) \right] \quad (1)$$

where we use a convenient notation<sup>2</sup> for the KL divergence:  $\text{KL}(a_t|x_t) = \mathbb{E}_{\pi(a_t|x_t)} [\log \frac{\pi(a_t|x_t)}{\pi_0(a_t|x_t)}]$ ,  $\gamma$  is the discount factor and  $\alpha$  is a hyperparameter controlling the relative contributions of both terms.  $\mathbb{E}_\tau[\cdot]$  is taken with respect to the distribution over trajectories defined by the agent policy and system dynamics:  $p(s_1) \prod_{t \geq 1} \pi(a_t|x_t) p(s_{t+1}|s_t, a_t)$ .

When optimized with respect to  $\pi$  the objective can be seen to trade off expected reward with closeness (in terms of KL) to  $\pi_0$ . This is also evident from the optimal  $\pi$  in eq. (1)

$$\pi^*(a_t|x_t) = \pi_0(a_t|x_t) \exp \frac{1}{\alpha} (Q^*(x_t, a_t) - V^*(x_t)) \quad (2)$$

$$Q^*(x_t, a_t) = r(s_t, a_t) + \gamma \mathbb{E}_{s_{t+1}|s_t, a_t} [V^*(x_{t+1})] \quad (3)$$

$$V^*(x_t) = \alpha \log \int \pi_0(a_t|x_t) \exp \frac{1}{\alpha} Q^*(x_t, a_t) da_t, \quad (4)$$

where  $Q^*(\cdot)$  and  $V^*(\cdot)$  are optimal action value and value functions of eq. (1); See (e.g. Rawlik et al., 2012; Fox et al.,

<sup>1</sup> We generally work with history dependent policies since we will consider restricting access to state information from policies (for information asymmetry), which may render fully observed MDPs effectively partially observed.

<sup>2</sup>In the following,  $\text{KL}(Y|X)$  always denotes  $\mathbb{E}_{\pi(Y|X)} [\log \frac{\pi(Y|X)}{\pi_0(Y|X)}]$  for arbitrary variables  $X$  and  $Y$ .

2016; Schulman et al., 2017a; Nachum et al., 2017) for derivations. We can thus think of  $\pi$  as a specialization of  $\pi_0$  that is obtained by tilting  $\pi_0$  towards high-value actions (as measured by the action value  $Q$ ). Several recent works have considered optimizing (1) when  $\pi_0$  is of a fixed and simple form. For instance, when  $\pi_0$  is chosen to be the uniform distribution the entropy-regularized objective is recovered (e.g. Ziebart, 2010; Fox et al., 2016; Haarnoja et al., 2017; Schulman et al., 2017a; Hausman et al., 2018). More interestingly, there are scenarios where available  $\pi_0$  can be used to inject detailed prior knowledge into the learning problem. In a transfer scenario  $\pi_0$  can be a *learned* object, and the KL term plays effectively the role of a shaping reward.

$\pi$  and  $\pi_0$  can also be co-optimized. In this case the relative parametric forms of  $\pi_0$  and  $\pi$  are of importance. The optimal  $\pi_0$  in eq. (1) is

$$\pi_0^*(a_t|x_t) = \arg \max_{\pi_0} \mathbb{E}_{\pi(a_t|x_t)} [\log \pi_0(a_t|x_t)], \quad (5)$$

which maximizes only terms in eq. (1) depending on  $\pi_0$ . Thus learning  $\pi_0$  can be seen as supervised learning where  $\pi_0$  is trained to match the history-conditional action sequences produced by  $\pi$ . It should be clear that  $\pi_0 = \pi$  is the optimal solution when  $\pi_0$  has sufficient capacity, and in this scenario the regularizing effect of  $\pi_0$  is lost. When the capacity of  $\pi_0$  is limited then  $\pi_0$  will be forced to generalize the behavior of  $\pi$ . For instance, (Teh et al., 2017) and (Galashov et al., 2019) consider a multitask scenario in which  $\pi$  is given task-identifying information, while  $\pi_0$  is not. As a result,  $\pi_0$  is forced to learn a common default behaviour across tasks, and this behaviour is then shareable across tasks to regularize  $\pi$ .

More generally, appropriate choices for the model classes of  $\pi_0$  and  $\pi$  will allow us to influence both the learning dynamics as well as the final solutions to eq. (1) and thus provide us with a rich means of injecting prior knowledge into the learning problem. This closely mirrors the discussion in the probabilistic modeling literature where the parametric form of a model will greatly influence its ability to generalize to unseen data, as well as the nature of the learned representation. (Galashov et al., 2019) focus on the information that  $\pi_0$  has access to. Their discussion suggested that restricting the information available to  $\pi_0$  improves generalization but also reduces the specificity of the modelled default behaviour.

## 3. Hierarchically structured policies

In this paper we focus on a complementary perspective. We explore how variations of the parametric forms of  $\pi_0$  and  $\pi$ , via the introduction of latent variables, give rise to hierarchically structured models with different inductive biases and generalization properties. In this section we discuss a particular instantiation of this idea and discuss the general framework in Appendix A.

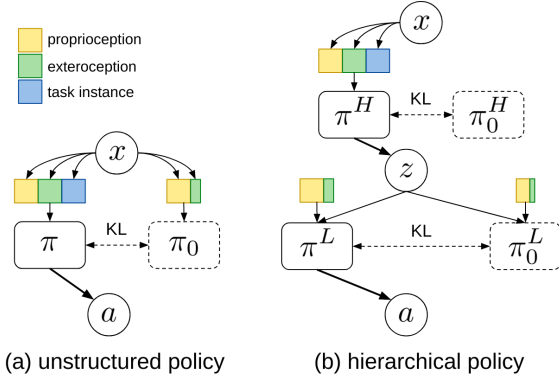


Figure 1. Diagram of the generic structure of the regularized KL-objective considered. (a) shows an unstructured policy, where information asymmetry (e.g. hiding task instance information) is exploited to induce a meaningful default policy  $\pi_0$  (Galashov et al., 2019); (b) shows the scenario when we use structured policies composed from high-level  $\pi^H$  and low-level  $\pi^L$  policies that communicate through the latent action  $z$ . Note that now different forms of information asymmetry can be employed. See text for details.

We consider multi-level representations of behaviour. In our experiments we instantiate a two level architecture in which the high-level decisions are concerned with task objectives but largely agnostic to details of actuation. The low-level control translates the high-level decisions into motor actions while being agnostic to task objectives. The resulting abstractions can exploit repetitive structures within or across tasks. As two use cases we consider (a) multi-task control where different tasks require similar motor-skills; as well as (b) a scenario where we aim to solve similar tasks with different actuation systems.

Conceptually policies are divided into high-level and low-level components which interact via auxiliary latent variables. Let  $z_t$  be a (continuous) latent variable for each time step  $t$  (we discuss alternative choices such as latent variables that are sampled infrequently in Appendices A and C). The agent policy is extended as  $\pi(a_t, z_t|x_t) = \pi^H(z_t|x_t)\pi^L(a_t|z_t, x_t)$  and likewise for the default policy  $\pi_0$ .  $z_t$  can be interpreted as a high-level or abstract action, taken according to the high-level (HL) controller  $\pi^H$ , and which is translated into low-level or motor action  $a_t$  by the low-level (LL) controller  $\pi^L$ . We extend the histories  $x_t$  and trajectories  $\tau$  to appropriately include  $z_t$ 's. As will be discussed in Section 5, structuring a policy into HL and LL controllers has been studied previously (e.g. Heess et al., 2016; Hausman et al., 2018; Haarnoja et al., 2018a; Merel et al., 2019), but the concept of default policy has not been widely explored in this context.

In case  $z_t$ 's can take on many values or are continuous, the objective (1) becomes intractable as the marginal distributions  $\pi(a_t|x_t)$  and  $\pi_0(a_t|x_t)$  in the KL divergence cannot be computed in closed form. As discussed in more detail

in Appendix A this problem can be addressed in different ways. For simplicity and concreteness we here assume that the latent variables in  $\pi$  and  $\pi_0$  have the same dimension and semantics. We can then construct a lower bound for the objective by using the following upper bound for the KL:

$$\text{KL}(a_t|x_t) \leq \text{KL}(z_t|x_t) + \mathbb{E}_{\pi(z_t|x_t)}[\text{KL}(a_t|z_t, x_t)], \quad (6)$$

which is tractably approximated using Monte Carlo sampling. The derivation is in Appendix C.1. Note that:

$$\text{KL}(z_t|x_t) = \text{KL}(\pi^H(z_t|x_t) \parallel \pi_0^H(z_t|x_t)) \quad (7)$$

$$\text{KL}(a_t|z_t, x_t) = \text{KL}(\pi^L(a_t|z_t, x_t) \parallel \pi_0^L(a_t|z_t, x_t)). \quad (8)$$

The resulting lower bound for the objective is:

$$\mathcal{L}(\pi, \pi_0) \geq \mathbb{E}_{\tau} \left[ \sum_{t \geq 1} \gamma^t r(s_t, a_t) - \alpha \gamma^t \text{KL}(z_t|x_t) - \alpha \gamma^t \text{KL}(a_t|z_t, x_t) \right], \quad (9)$$

where  $\tau$  is a trajectory that appropriately includes  $z_t$ 's. Full derivation including discount terms is in Appendix C.2. In this paper we consider eq. (9) as a main objective function.

### 3.1. Sharing low-level controllers

An advantage of the hierarchical structure of the policies is that it enables several options for partial parameter sharing, which when used in the appropriate context can make learning more statistically efficient. As a special case we consider sharing low-level controllers in both the agent and the default policy, i.e.  $\pi^L(a_t|z_t, x_t) = \pi_0^L(a_t|z_t, x_t)$ . This results in a new lower bound:

$$\mathcal{L}(\pi, \pi_0) \geq \mathbb{E}_{\tau} \left[ \sum_{t \geq 1} \gamma^t r(s_t, a_t) - \alpha \gamma^t \text{KL}(z_t|x_t) \right] \quad (10)$$

Note that this objective function is similar in spirit to current KL-regularized RL approaches discussed in Section 2, except that the KL divergence is between policies defined on abstract actions  $z_t$  as opposed to concrete actions  $a_t$ . The effect of this KL divergence is that it regularizes both the HL policies as well as the space of behaviours parameterised by the abstract actions. This special case of our framework reveals connection to (Goyal et al., 2019) as well, which motivated eq. (10) as an approximation of information bottleneck for learning a goal conditioned policy. In Section 6 and 7, we empirically demonstrate and discuss how sharing or separating low-level controllers can be useful in different learning scenarios.

### 3.2. Regularizing via information asymmetries

As discussed in (Galashov et al., 2019) restricting the information available to different policies is a powerful tool to force regularization and generalization. In our case we let

this information asymmetry be reflected also in the separation between HL and LL controllers (see Figure 1). Specifically we introduce a separation of concerns between  $\pi^L$  and  $\pi^H$  by providing full information only to  $\pi^H$  while information provided to  $\pi^L$  is limited. In our experiments we vary the information provided to  $\pi^L$ ; it receives body-specific (proprioceptive) information as well as different amounts of environment-related (exteroceptive) information. The task is only known to  $\pi^H$ . Hiding task specific information from the LL controller makes it easier to transfer across tasks. It forces  $\pi^L$  to focus on learning task agnostic behaviour, and to rely on the abstract actions selected by  $\pi^H$  to solve the task. Similarly, we hide task specific information from  $\pi_0^L$ , regardless of the parameter sharing strategy for the LL controllers. Since we also limit the information available to  $\pi_0^H$  (see section 3.3), this setup implements a similar default behaviour policy  $\pi_0(a_t|x_t)$  as in (Galashov et al., 2019), which can be derived by marginalizing the latents  $\int_{z_t} \pi_0^H(z_t|x_t)\pi_0^L(a_t|z_t, x_t)dz_t$ .

In the experiments we further consider transferring the HL controller across bodies, in situations where the abstract task is the same but the body changes. Here we additionally hide body-specific information from  $\pi^H$ , so that the HL controller is forced to learn body-agnostic behaviour.

### 3.3. Parametrizing the default policy

In our experiments we consider different formulations for the default policy. For LL default policy, we use identical parametric forms to implement  $\pi^L$  and  $\pi_0^L$ , regardless of the parameter sharing strategy. The specific form of LL controller depends on the experiments. The remaining freedom lies in the choice of the default HL controller  $\pi_0^H(z_t|x_t)$ , which may induce different inductive bias based on its parametric form. Here, we consider the following choices:

**Independent isotropic Gaussian** We define the default HL policy as  $\pi_0^H(z_t|x_t) = \mathcal{N}(z_t|0, 1)$ .

**AR(1) process**  $\pi_0^H(z_t|x_t) = \mathcal{N}(z_t|\alpha z_{t-1}, \sqrt{1-\alpha^2})$ , i.e. the default HL policy is a first-order auto-regressive process with a fixed parameter  $0 \leq \alpha < 1$  chosen to ensure a marginal distribution  $\mathcal{N}(0, 1)$ . This allows for more structured temporal dependence among the abstract actions.

**Learned AR prior** Similar to the AR(1) process this default HL policy allows  $z_t$  to depend on  $z_{t-1}$  but now the high-level default policy is a Gaussian distribution with mean and variance that are learned functions of  $z_{t-1}$  with parameters  $\phi$ :  $\pi_0^H(z_t|x_t) = \mathcal{N}(z_t|\mu_\phi(z_{t-1}), \sigma_\phi^2(z_{t-1}))$ .

## 4. Algorithm

There are different instantiations of the proposed method based on several algorithmic choices. In case  $\pi_0^H$  has learn-

---

### Algorithm 1 Simple actor-critic algorithm

---

Flat (HL+LL) policy:  $\pi_\theta(a_t|\epsilon_t, x_t)$ , parameter  $\theta$   
 HL policy:  $\pi_\theta^H(z_t|x_t)$ , sample  $z_t = g(f_\theta^H(x_t), \epsilon_t)$   
 Default policy:  $\pi_{0,\phi}^H(z_t|x_t)$ ,  $\pi_{0,\phi}^L(a_t|z_t, x_t)$ , parameter  $\phi$   
 Q-function:  $Q_\psi(a_t, z_t, x_t)$ , parameter  $\psi$   
**repeat**  
   **for**  $t = 0, K, 2K, \dots T$  **do**  
     Rollout trajectory:  $\tau_{t:t+K} = (s_t, a_t, r_t, \dots, r_{t+K})$   
     Sample latent:  $\epsilon_{t'} \sim \rho(\epsilon)$ ,  $z_{t'} = g(f_\theta^H(x_{t'}), \epsilon_{t'})$   
     Compute KL:  $\widehat{KL}_{t'} = \text{KL}(z|x_{t'}) + \text{KL}(a|z_{t'}, x_{t'})$   
     Bootstrap:  $\hat{V} = \mathbb{E}_\pi Q(a, z_{t+K}, x_{t+K}) - \alpha \widehat{KL}_{t+K}$   
     Estimate Q target:  $\hat{Q}_{t'} = \sum_{i=t'}^{t'+K-1} (r_i - \alpha \widehat{KL}_i) + \hat{V}$   
     Policy loss:  $\hat{L}_\pi = \sum_{i=t}^{t+K-1} \mathbb{E}_\pi Q(a, z_i, x_i) - \alpha \widehat{KL}_i$   
     Q-value loss:  $\hat{L}_Q = \sum_{i=t}^{t+K-1} \|\hat{Q}_i - Q(a, z_i, x_i)\|^2$   
     Default policy loss:  $\hat{L}_{\pi_0} = \sum_{i=t}^{t+K-1} \widehat{KL}_i$   
      $\theta \leftarrow \theta + \beta_\pi \nabla_\theta \hat{L}_\pi$      $\phi \leftarrow \phi + \beta_{\pi_0} \nabla_\phi \hat{L}_{\pi_0}$   
      $\psi \leftarrow \psi - \beta_Q \nabla_\psi \hat{L}_Q$   
   **end for**  
**until**

---

able parameters (learned AR prior) or  $\pi_0^L$  is not shared, we jointly optimize the default policy and the agent’s policy, while the agent’s policy is regularized by a *target default policy*, which is periodically updated to a new default policy. The objective for the HL default policy is similar to distillation (Parisotto et al., 2016; Rusu et al., 2016) or supervised learning, where HL controller  $\pi^H$  defines the data distribution. Note that due to the particular way we lower bound the KL (section 3) the supervised step remains unproblematic despite the presence of the latent variables in  $\pi_0$ .<sup>3</sup>

To optimize the hierarchical policy, we follow a strategy similar to Heess et al. (2016) and reparameterize  $z_t \sim \pi^H(z_t|x_t)$  as  $z_t = f^H(x_t, \epsilon_t)$ , where  $\epsilon_t \sim \rho(\epsilon_t)$  is a fixed noise distribution and  $f^H(\cdot)$  is a deterministic function. In practice this means that the hierarchical policy can be treated as a flat policy  $\pi(a_t|\epsilon_t, x_t) = \pi^L(a_t|f^H(x_t, \epsilon_t), x_t)$ . We can employ different algorithms to optimize this policy. As an example, Algorithm 1 provides the pseudo-code for a simple actor-critic algorithm; in the experiments we use different formulations depending on the environment.

In continuous control experiments, we employ SVG(0) (Heess et al., 2015) augmented with experience replay to train the agents. We reparameterize the flat policy  $\pi(a_t|\epsilon_t, x_t)$  and optimize it by backpropagating the gradient from an action value function. The action value function is optimized to match a target action value estimated by Retrace (Munos et al., 2016), which provides low variance estimate of action value from K-step windows of off-policy trajectories.

<sup>3</sup>We discuss alternative schemes in Appendix A.



For discrete action spaces we adapt IMPALA (Espeholt et al., 2018), a distributed actor critic algorithm with off-policy correction. We estimate the gradient of the flat policy  $\pi(a_t|\epsilon_t, x_t)$  as  $(q_t - b_t)\nabla_{\theta}\pi(a_t|\epsilon_t, x_t)$ , where  $q_t$  is the action value estimate and  $b_t$  is a baseline. We use a learned value function as  $b_t$  and to estimate  $q_t$  based on V-trace (Espeholt et al., 2018), which provides low variance estimate of  $q_t$  from off-policy trajectories. The off-policy trajectories are buffered by a queue of size equal to one mini-batch to ensure the trajectories are close to the current policy.

All algorithms are implemented in a distributed setup (Espeholt et al., 2018; Riedmiller et al., 2018) where multiple actors are used to collect trajectories and a single learner is used to optimize model parameters. Similarly to other KL-regularized RL approaches (e.g. Teh et al., 2017; Galashov et al., 2019), we additionally regularize the entropy of  $\pi^L$  to encourage exploration. More details about the learning algorithms are in Appendix B.

## 5. Related Work

Entropy regularized reinforcement learning (RL), also known as maximum entropy RL (Ziebart, 2010; Kappen et al., 2012; Toussaint, 2009) is a special case of KL regularized RL. This framework connects probabilistic inference and sequential decision making problems. Recently, this idea has been adapted to deep reinforcement learning (Fox et al., 2016; Schulman et al., 2017a; Nachum et al., 2017; Haarnoja et al., 2017; Hausman et al., 2018; Haarnoja et al., 2018b). Another instance of KL regularized RL includes trust region based methods (Schulman et al., 2015; 2017b; Wang et al., 2017; Abdolmaleki et al., 2018). They use KL divergence between new policy and old policy as a trust region constraints for conservative policy update.

Introducing a parameterized default policy provides a convenient way to transfer knowledge or regularize the policy. Schmitt et al. (2018) use a pretrained policy as the default policy; other works jointly learn the policy and default policy to capture reusable behaviour from experience (Teh et al., 2017; Czarnecki et al., 2018; Galashov et al., 2019; Grau-Moya et al., 2019). To retain the role of default policy as a regularizer, it has been explored to restrict its input (Galashov et al., 2019; Grau-Moya et al., 2019), parametric form (Czarnecki et al., 2018) or to share it across different contexts (Teh et al., 2017; Ghosh et al., 2018).

Another closely related regularization for RL is using information bottleneck (Tishby & Polani, 2011; Still & Precup, 2012; Rubin et al., 2012; Ortega & Braun, 2013; Tiomkin & Tishby, 2017). Galashov et al. (2019) discussed the relation between information bottleneck and KL regularized RL. Strouse et al. (2018) learn to hide or reveal information for future use in multi-agent cooperation or competition. Goyal

et al. (2019) consider identifying bottleneck states based on objective similar to eq. (10), which is a special case of our framework, and using it for transfer. However their setting is differently motivated, and so is their objective. For example, they use the *positive KL* between pretrained HL controllers as an exploration bonus, to learn a new related task. On the other hand we are interested in transferring the same behaviour policy to a different body. For this we rely on the *negative KL* as intrinsic rewards, as a signal whether the LL controller executed the latent action set by HL controller.

The hierarchical RL literature (Dayan & Hinton, 1993; Parr & Russell, 1998; Sutton et al., 1999) has studied hierarchy extensively as a means to introduce inductive bias. Among various ways (Sutton et al., 1999; Bacon et al., 2017; Vezhnevets et al., 2017; Nachum et al., 2018; 2019; Xie et al., 2018), our approach resembles Heess et al. (2016); Hausman et al. (2018); Haarnoja et al. (2018a); Merel et al. (2019), in that a HL controller modulates a LL controller through a continuous channel. For learning the LL controller, imitation learning (Fox et al., 2017; Krishnan et al., 2017; Merel et al., 2019), unsupervised learning (Gregor et al., 2017; Eysenbach et al., 2019) and meta learning (Frans et al., 2018) have been employed. Similar to our approach, (Heess et al., 2016; Florensa et al., 2017; Hausman et al., 2018) use a pretraining task to learn a reusable LL controller. However, the concept of a default policy has not been widely explored in this context.

Works that transfer knowledge across different bodies include (Devin et al., 2017; Gupta et al., 2017; Sermanet et al., 2017; Xie et al., 2018). Devin et al. (2017) mixes and matches modular task and body policies for zero-shot generalization to unseen combination. Gupta et al. (2017); Sermanet et al. (2017) learn a common representation space to align poses from different bodies. Xie et al. (2018) transfer the HL controller in a hierarchical agent, where the LL controller is learned with an intrinsic reward based on goals in state space. This approach, however, requires careful design of the goal space and the intrinsic reward.

## 6. Experiments

We evaluate our method in several environments with continuous action space and states. We consider a set of structured, sparse reward tasks that can be executed by multiple bodies with different degrees of freedom. The tasks and bodies are illustrated in Figure 2.

We consider task distributions that are designed such that their solutions exhibit significant overlap in trajectory space so that transfer can reasonably be expected. They are further designed to contain instances of variable difficulty and hence provide a natural curriculum. **Go to 1 of K targets:** In this task the agent receives a sparse reward on reaching a

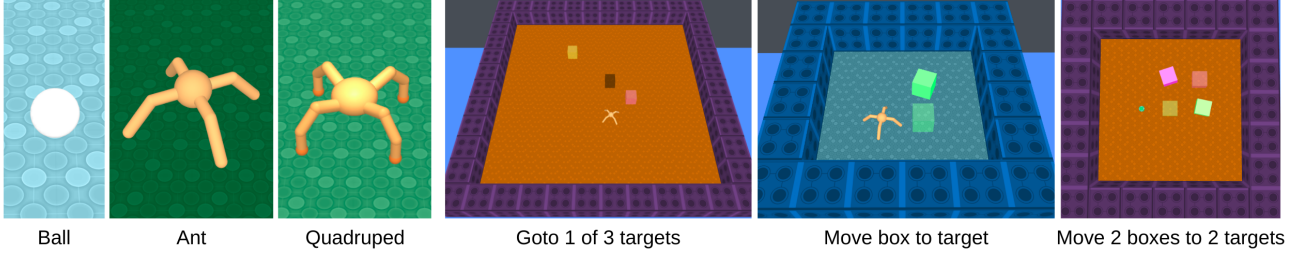


Figure 2. **Bodies and tasks for continuous control experiments.** Left: All considered bodies. Right: Example tasks.

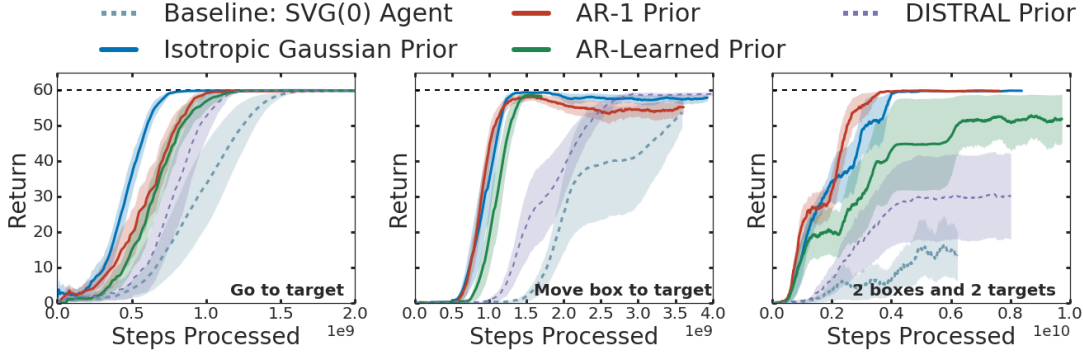


Figure 3. **Speed up for learning complex tasks from scratch.** Left: Go to 1 of 3 targets with the Ant. Center: Move a single box to a single target with the Ant. Right: Move 2 boxes to 2 targets with the Ball. The proposed model is denoted with the type of HL default policy: Isotropic Gaussian, AR-1, AR-Learned.

specific target among  $K$  locations. The egocentric locations of each of the targets and the goal target index are provided as observations. **Move  $K$  boxes to  $K$  targets:** the goal is to move one of  $K$  boxes to one of  $K$  targets (the positions of which are randomized) as indicated by the environment. **Move heavier box:** variants of move  $K$  boxes to  $K$  targets with heavier boxes. **Gather boxes:** the agent needs to move two boxes such that they are in contact with each other. We also consider **Move box and go to target**, in which the agent is required to move the box to one target and then go to a different target in a single episode.

We use three different bodies: Ball, Ant, and Quadruped. Ball and Ant have been used in several previous works (Heess et al., 2017; Xie et al., 2018; Galashov et al., 2019), and we introduce the Quadruped as an alternative to the Ant. The **Ball** is a body with 2 actuators for moving forward or backward and turning left or right. The **Ant** is a body with 4 legs and 8 actuators, which moves its legs to walk and to interact with objects. The **Quadruped** is similar to the Ant, but with 12 actuators. Each body is characterized by a different set of proprioceptive (proprio) features. Further details of the tasks and bodies are in Appendix E.

### 6.1. Experimental setting

Throughout the experiments, we use 32 actors to collect trajectories and a single learner to optimize the model. We plot average episode return with respect to the number of

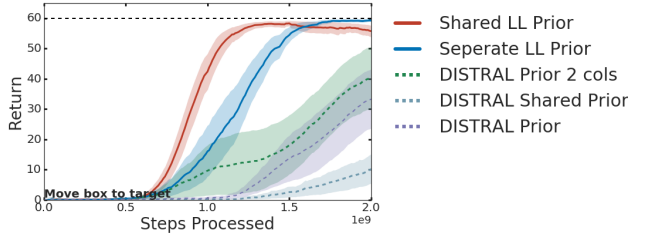


Figure 4. **Analysis on learning from scratch result.** Move box to target, Ant, AR-1 process.

steps processed by the learner. Note that the number of steps is different from the number of agent’s interaction with environment, because the collected trajectories are processed multiple times by a centralized learner to update model parameters. Hyperparameters, including KL cost and action entropy regularization cost, are optimized on a per-task basis. Details are provided in Appendices F and G.

### 6.2. Learning from scratch experiments

We first study whether KL regularization with the proposed structure and parameterization benefits end-to-end learning. As baselines, we use a policy with entropy regularization (SVG-0) and a KL regularized policy with unstructured default policy similar to Galashov et al. (2019); Teh et al. (2017) (DISTRAL prior). As described in Section 3 we employ hierarchical structure with shared LL components (Shared LL prior) and with separate LL components (Sepa-

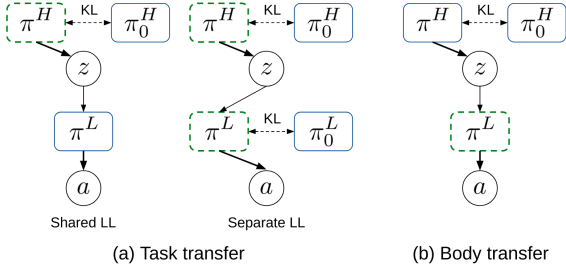


Figure 5. **Transfer learning scenarios.** The blue boxes denote modules that are transferred and fixed, and the green dotted boxes denote modules learned from scratch.

rate LL prior). Unless otherwise stated, we use Shared LL prior as our default hierarchical model. The HL controller receives full information while the LL controller (and hence the default policy) receives proprioceptive information plus the positions of the box(es) as indicated. The same information asymmetry is applied to the DISTRAL prior i.e. the default policy receives proprioception plus box positions as inputs. We explore multiple HL default policies including Isotropic Gaussian, AR(1) process, and learned AR prior.

Figure 3 illustrates the results of the experiment. Our main finding is that the KL regularized objective significantly speeds up learning of complex tasks, and that the hierarchical approach provides an advantage over the flat, DISTRAL formulation. The gap increases for more challenging tasks (e.g. move 2 boxes to 2 targets). For analysis, we compare different combinations of hierarchical structure and parameter sharing strategies. As baselines using parameter sharing without hierarchy, we introduce **DISTRAL prior 2 cols** and **DISTRAL shared prior**, which are variants of DISTRAL prior with different parameter sharing strategies. Details of these baselines are explained in Appendix F.2. The result in Figure 4 shows that both hierarchical structure and partial parameter sharing, introduced with the proposed framework, are important to speed up learning.

## 7. Transfer Learning

The hierarchical structure introduces a modularity of the policy and default policy, which can be utilized for transfer learning. We consider two transfer scenarios (see Figure 5): 1) task transfer where we reuse the learned default policy to solve novel tasks with different goals, and 2) body transfer, where reusing the body agnostic HL controller and default policy transfers the goal directed behaviour to another body.

### 7.1. Task transfer

We consider transfer between task distributions whose solutions exhibit significant shared structure, e.g. because solution trajectories can be produced by a common set of skills or repetitive behaviour. If the default policy can capture

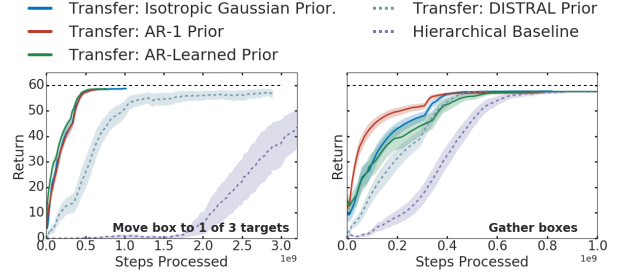


Figure 6. **Task transfer summary.** **Left:** From move box to target to move box to 1 of 3 targets with Ant. Box position and proprioception are given to LL controller. **Right:** From move 2 boxes to 2 targets to congregate boxes with Ball.

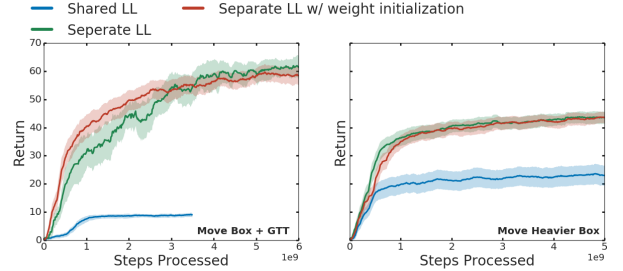


Figure 7. **Analysis on task transfer results.** **Left:** From move box to target task to move box and go to target with Ant, AR-1. **Right:** From move box to target to move heavier box with Ant, AR-1. In all cases, we use shared LL prior during pretraining.

and transfer this reusable structure it will facilitate learning similar tasks. Transfer then involves specializing the default behavior to the needs of the target task (e.g. by directing locomotion towards a goal).

For task transfer, we reuse pretrained goal agnostic components, including the HL default policy  $\pi_0^H$  and the LL default policy  $\pi_0^L$ , and learn a new HL controller  $\pi^H$  and optionally learn a new LL controller  $\pi^L$  for a target task (see Figure 5a). In general, we set the LL controller  $\pi^L$  identical to the LL default policy (Shared LL), but for some tasks we allow  $\pi^L$  to diverge from  $\pi_0^L$  (Separate LL). In case of Shared LL, similarly e.g. to Heess et al. (2016); Hausman et al. (2018), the new HL controller  $\pi^H$  learns to manipulate the LL controller  $\pi^L$  by modulating and interpolating the latent space, while being regularized by  $\pi_0^H$ . Compared to Galashov et al. (2019), which also attempts to transfer default behaviour learned on a different task, in this work we exploit the structure of  $\pi^0$  and  $\pi$ . In particular, in case LL policy and default policy are parameterized identically, we could either share parameter (Shared LL) or initialize LL policy with the pretrained parameters of LL default policy (Separate LL with weight initialization) to exploit pretrained goal agnostic behaviour even in the initial phase of learning.

In the experiments we introduce two baselines. The first baseline, the identical model learned from scratch (Hierarchical Agent), allows us to assess the benefit of transfer. The

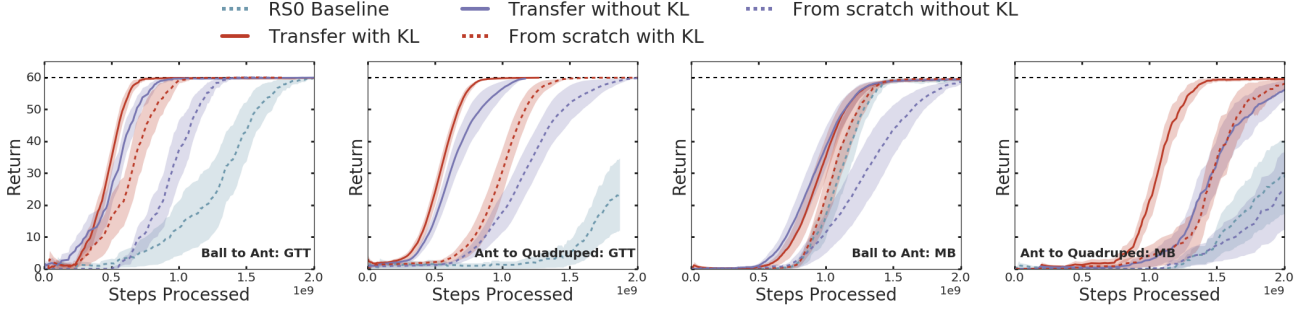


Figure 8. **Body transfer with the AR-1 Prior.** Column 1: Ball to Ant, Go to 1 of 3 targets. Column 2: Ball to Ant, Move box to target. Column 3: Ant to Quadraped, Go to 1 of 3 targets. Column 4: Ant to Quadraped, Move box to target.

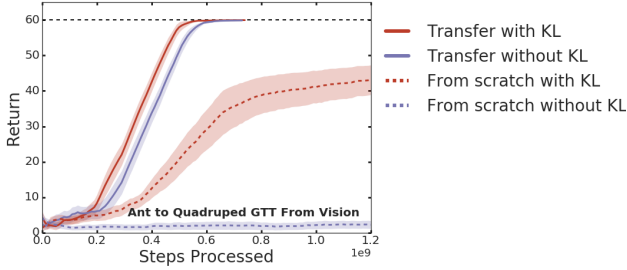


Figure 9. **Body transfer from vision with the AR-1 Prior.** Ant to Quadraped, Go to 1 of 3 targets. Task information is provided by egocentric vision.

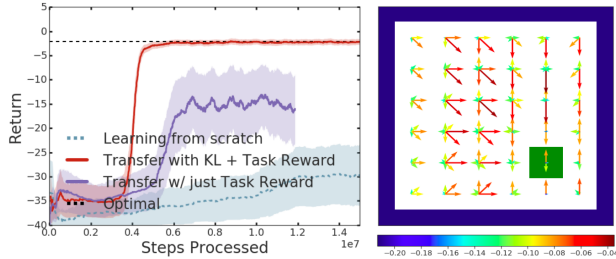


Figure 10. **Body transfer in 2D grid world.** Left Transfer from 1-step to 8-step body. Right KL reward visualization. The size and the color of arrows denotes KL reward (negative KL) for corresponding agents' movement.

second baseline is a DISTRAL-style prior, i.e. we transfer a pretrained unstructured default policy to regularize the policy for the target task. This second baseline provides an indication whether the hierarchical policy structure is beneficial for transfer. Additionally, we compare different types of HL default policies. Specifics of the experiments including the information provided to HL and LL are provided in Appendix E.

Figure 6 illustrates the result of task transfer. Overall, transferring the pretrained default policy brings significant benefits when learning related tasks. Furthermore the hierarchical architecture which facilitates parameter reuse performs better than the DISTRAL prior regardless of type of HL default policy. While sharing the LL is effective for trans-

fer between tasks with significant overlap, allowing the LL *policy* to diverge from the LL *default policy* as in eq. (9) is useful in some cases. Figure 7 illustrates the result on task transfer scenarios requiring adaptation of skills. Here the LL policy is only initialized and soft-constrained to the behavior of the LL default policy (via the KL term in eq. (9)) which allows adapting the LL skills as required for target task.

## 7.2. Body transfer

Our formulation can also be used for transfer between different bodies which share common behaviour structures for the same task distribution. To transfer the HL structure of a goal-specific behaviour, we reuse the pretrained body-agnostic components, HL controller  $\pi^H$  and the default policy  $\pi_0^H$ . We learn a new body-specific LL controller  $\pi^L$ , which is assumed to be shared with LL default controller  $\pi_0^L$  (see Figure 5b). The transferred HL components provide goal-specific behaviour actuated on the latent space, which can then be instantiated by learning a new LL controller.

The main challenge of transferring task knowledge across bodies is how to interpret the latent actions. The HL controller  $\pi^H$  provides abstract instructions for solving a task but it is unknown how they should be instantiated on the new body. Furthermore, rewarding the LL controller in order to learn the semantics of the latent code is problematic, as these semantics are not available to us. To address this challenge, we optimize eq. (10) during transfer; it provides a dense reward signal based on the negative KL divergence. Using KL of the HL components during transfer looks similar to Goyal et al. (2019). However its interpretation and behaviour is quite different. Goyal et al. (2019) rely on the *positive KL* between HL controllers as an exploration bonus, trying to get the agent to explore the new task (in the transfer phase). On the contrary we rely on *negative KL*, which encourages the HL controller to be close to the default policy. In our scenario the *negative KL* is an intrinsic reward telling us if the LL controller executed the latent action properly so that HL controller could behave in a habitual way.



We explore this body transfer setup both in discrete and continuous environments. We compare performance to learning the hierarchical policy from scratch and analyze the effects of the KL regularization. The experimental setup in the continuous case is the same as before, and Figure 8 provides results for different types of bodies and tasks. Generally transferring the HL component and relying on both the task reward and the KL term as a dense shaping reward signal for LL controller works best in these settings. As illustrated in Figure 9, this trend is also apparent when using egocentric vision as observation input.

In the discrete case, we construct a **discrete go to target** task in a 2D grid world. An agent and goal are randomly placed in an  $8 \times 8$  grid and the agent is rewarded for reaching the goal. The body agnostic task observation is the global x, y coordinates of the agent and goal. The different bodies in this case must take different numbers of actions to achieve an actual step in the grid. For instance the 4-step body needs to take 4 consecutive actions in the same direction to move forward by one step in that direction. We assume that the latent  $z_t$  is sampled every  $n$  steps, where  $n$  is the number of actions required to take a step. Details for models in which latent variables are sampled with a period  $> 1$  are provided in Appendix B. The environment is described in Appendix E.

Figure 10 illustrates the result for transferring behavior from the 1-step to the 8-step body with AR-learned prior. (We were only able to solve the challenging 8-step version through body transfer with a KL reward.) In Figure 10, we visualize the negative KL divergence (KL reward) along the agent’s movement in every location of the grid. The size and the colour of arrows denotes the expected KL reward. This illustrates that the KL reward forms a vector field that guides the agent toward the goal, which provides a dense reward signal when transferring to a new body. This observation explains the gain from KL regularization, which can lead to faster learning and improve asymptotic performance.

## 8. Discussion

In this work we explore how hierarchical structure can be introduced in KL-regularized RL using latent variables, how inductive biases can be introduced in these structures via information asymmetry and parameter sharing, and how this can lead to specialization of policy components and induce semantically meaningful latent representations. We show that the resulting structures can be exploited efficiently at transfer time, where either the HL component or the LL component can be completely transferred to new tasks. Furthermore, in the case of body transfer (where the LL component needs to be relearned), the KL term between the HL components  $\pi^H$  and  $\pi_0^H$  acts as a dense reward signal guiding learning for the LL component.

Overall, we believe that the framework of KL-regularized RL as probabilistic modelling offers complex mechanisms for introducing prior knowledge, and is fertile grounds for advancing RL algorithms. Appendix A describes the framework in further generality than explored here.

## References

- Abdolmaleki, A., Springenberg, J. T., Tassa, Y., Munos, R., Heess, N., and Riedmiller, M. Maximum a posteriori policy optimisation. In *International Conference on Learning Representations*, 2018.
- Agakov, F. V. and Barber, D. An auxiliary variational method. In *Neural Information Processing, 11th International Conference, ICONIP 2004, Calcutta, India, November 22-25, 2004, Proceedings*, pp. 561–566, 2004.
- Bacon, P.-L., Harb, J., and Precup, D. The option-critic architecture. In *Thirty-First AAAI Conference on Artificial Intelligence*, 2017.
- Czarnecki, W., Jayakumar, S., Jaderberg, M., Hasenclever, L., Teh, Y. W., Heess, N., Osindero, S., and Pascanu, R. Mix & match agent curricula for reinforcement learning. In *Proceedings of the 35th International Conference on Machine Learning*, 2018.
- Dayan, P. and Hinton, G. E. Feudal reinforcement learning. In *Advances in neural information processing systems*, pp. 271–278, 1993.
- Devin, C., Gupta, A., Darrell, T., Abbeel, P., and Levine, S. Learning modular neural network policies for multi-task and multi-robot transfer. In *IEEE International Conference on Robotics and Automation (ICRA)*, pp. 2169–2176. IEEE, 2017.
- Espeholt, L., Soyer, H., Munos, R., Simonyan, K., Mnih, V., Ward, T., Doron, Y., Firoiu, V., Harley, T., Dunning, I., et al. Impala: Scalable distributed deep-rl with importance weighted actor-learner architectures. In *Proceedings of the 35th International Conference on Machine Learning*, 2018.
- Eysenbach, B., Gupta, A., Ibarz, J., and Levine, S. Diversity is all you need: Learning skills without a reward function. In *International Conference on Learning Representations*, 2019.
- Florensa, C., Duan, Y., and Abbeel, P. Stochastic neural networks for hierarchical reinforcement learning. In *International Conference on Learning Representations*, 2017.
- Fox, R., Pakman, A., and Tishby, N. Taming the noise in reinforcement learning via soft updates. In *Proceedings of the Thirty-Second Conference on Uncertainty in Artificial Intelligence*, pp. 202–211. AUAI Press, 2016.

- Fox, R., Krishnan, S., Stoica, I., and Goldberg, K. Multi-level discovery of deep options. *CoRR*, abs/1703.08294, 2017. URL <http://arxiv.org/abs/1703.08294>.
- Frans, K., Ho, J., Chen, X., Abbeel, P., and Schulman, J. Meta learning shared hierarchies. In *International Conference on Learning Representations*, 2018.
- Galashov, A., Jayakumar, S., Hasenclever, L., Tirumala, D., Schwarz, J., Desjardins, G., Czarnecki, W. M., Teh, Y. W., Pascanu, R., and Heess, N. Information asymmetry in KL-regularized RL. In *International Conference on Learning Representations*, 2019.
- Ganin, Y., Kulkarni, T., Babuschkin, I., Eslami, S. M. A., and Vinyals, O. Synthesizing programs for images using reinforced adversarial learning. In *Proceedings of the 35th International Conference on Machine Learning*, pp. 1666–1675, 2018.
- Ghosh, D., Singh, A., Rajeswaran, A., Kumar, V., and Levine, S. Divide-and-conquer reinforcement learning. In *International Conference on Learning Representations*, 2018.
- Goyal, A., Islam, R., Strouse, D., Ahmed, Z., Larochelle, H., Botvinick, M., Levine, S., and Bengio, Y. Transfer and exploration via the information bottleneck. In *International Conference on Learning Representations*, 2019.
- Grau-Moya, J., Leibfried, F., and Vrancx, P. Soft q-learning with mutual-information regularization. In *International Conference on Learning Representations*, 2019.
- Gregor, K., Rezende, D. J., and Wierstra, D. Variational intrinsic control. In *International Conference on Learning Representations*, 2017.
- Gupta, A., Devin, C., Liu, Y., Abbeel, P., and Levine, S. Learning invariant feature spaces to transfer skills with reinforcement learning. In *International Conference on Learning Representations*, 2017.
- Haarnoja, T., Tang, H., Abbeel, P., and Levine, S. Reinforcement learning with deep energy-based policies. In *International Conference on Machine Learning*, pp. 1352–1361, 2017.
- Haarnoja, T., Hartikainen, K., Abbeel, P., and Levine, S. Latent space policies for hierarchical reinforcement learning. In *Proceedings of the 35th International Conference on Machine Learning*, pp. 1851–1860, 2018a.
- Haarnoja, T., Zhou, A., Abbeel, P., and Levine, S. Soft actor-critic: Off-policy maximum entropy deep reinforcement learning with a stochastic actor. In *Proceedings of the 35th International Conference on Machine Learning*, pp. 1861–1870, 2018b.
- Hausman, K., Springenberg, J. T., Wang, Z., Heess, N., and Riedmiller, M. Learning an embedding space for transferable robot skills. In *International Conference on Learning Representations*, 2018.
- Heess, N., Wayne, G., Silver, D., Lillicrap, T., Erez, T., and Tassa, Y. Learning continuous control policies by stochastic value gradients. In *Advances in Neural Information Processing Systems*, 2015.
- Heess, N., Wayne, G., Tassa, Y., Lillicrap, T., Riedmiller, M., and Silver, D. Learning and transfer of modulated locomotor controllers. *arXiv preprint arXiv:1610.05182*, 2016.
- Heess, N., Tirumala, D., Sriram, S., Lemmon, J., Merel, J., Wayne, G., Tassa, Y., Erez, T., Wang, Z., Eslami, A., Riedmiller, M., et al. Emergence of locomotion behaviours in rich environments. *arXiv preprint arXiv:1707.02286*, 2017.
- Johnson, M., Duvenaud, D. K., Wiltchko, A., Adams, R. P., and Datta, S. R. Composing graphical models with neural networks for structured representations and fast inference. In *Advances in Neural Information Processing Systems 29*, pp. 2946–2954, 2016.
- Kappen, H. J., Gómez, V., and Opper, M. Optimal control as a graphical model inference problem. *Machine learning*, 87(2):159–182, 2012.
- Krishnan, S., Fox, R., Stoica, I., and Goldberg, K. DDCO: discovery of deep continuous options for robot learning from demonstrations. *CoRR*, abs/1710.05421, 2017. URL <http://arxiv.org/abs/1710.05421>.
- Levine, S., Finn, C., Darrell, T., and Abbeel, P. End-to-end training of deep visuomotor policies. *The Journal of Machine Learning Research*, 17(1):1334–1373, 2016.
- Lillicrap, T. P., Hunt, J. J., Pritzel, A., Heess, N., Erez, T., Tassa, Y., Silver, D., and Wierstra, D. Continuous control with deep reinforcement learning. In *International Conference on Learning Representations*, 2016.
- Merel, J., Hasenclever, L., Galashov, A., Ahuja, A., Pham, V., Wayne, G., Teh, Y. W., and Heess, N. Neural probabilistic motor primitives for humanoid control. In *International Conference on Learning Representations*, 2019.
- Mnih, V., Kavukcuoglu, K., Silver, D., Rusu, A. A., Veness, J., Bellemare, M. G., Graves, A., Riedmiller, M., Fidjeland, A. K., Ostrovski, G., et al. Human-level control through deep reinforcement learning. *Nature*, 518(7540): 529, 2015.

- Mnih, V., Badia, A. P., Mirza, M., Graves, A., Lillicrap, T., Harley, T., Silver, D., and Kavukcuoglu, K. Asynchronous methods for deep reinforcement learning. In *International conference on machine learning*, pp. 1928–1937, 2016.
- Munos, R., Stepleton, T., Harutyunyan, A., and Bellemare, M. Safe and efficient off-policy reinforcement learning. In *Advances in Neural Information Processing Systems*, 2016.
- Nachum, O., Norouzi, M., Xu, K., and Schuurmans, D. Bridging the gap between value and policy based reinforcement learning. In *Advances in Neural Information Processing Systems*, pp. 2775–2785, 2017.
- Nachum, O., Gu, S. S., Lee, H., and Levine, S. Data-efficient hierarchical reinforcement learning. In *Advances in Neural Information Processing Systems 31*, pp. 3307–3317, 2018.
- Nachum, O., Gu, S., Lee, H., and Levine, S. Near-optimal representation learning for hierarchical reinforcement learning. In *International Conference on Learning Representations*, 2019.
- OpenAI. Openai five. <https://blog.openai.com/openai-five/>, 2018.
- OpenAI, Andrychowicz, M., Baker, B., Chociej, M., Jozefowicz, R., McGrew, B., Pachocki, J., Petron, A., Plappert, M., Powell, G., Ray, A., et al. Learning dexterous in-hand manipulation. *arXiv preprint arXiv:1808.00177*, 2018.
- Ortega, P. A. and Braun, D. A. Thermodynamics as a theory of decision-making with information-processing costs. *Proceedings of the Royal Society A: Mathematical, Physical and Engineering Sciences*, 469(2153):20120683, 2013.
- Parisotto, E., Ba, J. L., and Salakhutdinov, R. Actor-mimic: Deep multitask and transfer reinforcement learning. In *International Conference on Learning Representations*, 2016.
- Parr, R. and Russell, S. J. Reinforcement learning with hierarchies of machines. In *Advances in neural information processing systems*, pp. 1043–1049, 1998.
- Rawlik, K., Toussaint, M., and Vijayakumar, S. On stochastic optimal control and reinforcement learning by approximate inference. In *Robotics: science and systems*, volume 13, pp. 3052–3056, 2012.
- Rennie, S. J., Marcheret, E., Mroueh, Y., Ross, J., and Goel, V. Self-critical sequence training for image captioning. In *Proceedings of the IEEE Conference on Computer Vision and Pattern Recognition*, pp. 7008–7024, 2017.
- Riedmiller, M., Hafner, R., Lampe, T., Neunert, M., De-grave, J., van de Wiele, T., Mnih, V., Heess, N., and Springenberg, J. T. Learning by playing solving sparse reward tasks from scratch. In *Proceedings of the 35th International Conference on Machine Learning*, pp. 4344–4353, 2018.
- Rubin, J., Shamir, O., and Tishby, N. Trading value and information in mdps. *Decision Making with Imperfect Decision Makers*, pp. 57–74, 2012.
- Rusu, A. A., Colmenarejo, S. G., Gulcehre, C., Desjardins, G., Kirkpatrick, J., Pascanu, R., Mnih, V., Kavukcuoglu, K., and Hadsell, R. Policy distillation. In *International Conference on Learning Representations*, 2016.
- Salimans, T., Kingma, D. P., and Welling, M. Markov Chain Monte Carlo and Variational Inference: Bridging the Gap. *ArXiv e-prints*, October 2014.
- Schmitt, S., Hudson, J. J., Zidek, A., Osindero, S., Doersch, C., Czarnecki, W. M., Leibo, J. Z., Kuttler, H., Zisserman, A., Simonyan, K., et al. Kickstarting deep reinforcement learning. *arXiv preprint arXiv:1803.03835*, 2018.
- Schulman, J., Levine, S., Moritz, P., Jordan, M., and Abbeel, P. Trust region policy optimization. In *Proceedings of the 32nd International Conference on International Conference on Machine Learning-Volume 37*, pp. 1889–1897. JMLR. org, 2015.
- Schulman, J., Chen, X., and Abbeel, P. Equivalence between policy gradients and soft q-learning. *arXiv preprint arXiv:1704.06440*, 2017a.
- Schulman, J., Wolski, F., Dhariwal, P., Radford, A., and Klimov, O. Proximal policy optimization algorithms. *arXiv preprint arXiv:1707.06347*, 2017b.
- Sermanet, P., Lynch, C., Hsu, J., and Levine, S. Time-contrastive networks: Self-supervised learning from multi-view observation. In *Proceedings of the IEEE Conference on Computer Vision and Pattern Recognition Workshops*, pp. 14–15, 2017.
- Silver, D., Huang, A., Maddison, C. J., Guez, A., Sifre, L., Van Den Driessche, G., Schrittwieser, J., Antonoglou, I., Panneershelvam, V., Lanctot, M., et al. Mastering the game of go with deep neural networks and tree search. *nature*, 529(7587):484, 2016.
- Still, S. and Precup, D. An information-theoretic approach to curiosity-driven reinforcement learning. *Theory in Biosciences*, 131(3):139–148, 2012.
- Strouse, D., Kleiman-Weiner, M., Tenenbaum, J., Botvinick, M., and Schwab, D. J. Learning to share and hide intentions using information regularization. In *Advances*

- in *Neural Information Processing Systems*, pp. 10270–10281, 2018.
- Sutton, R. S., Precup, D., and Singh, S. Between mdps and semi-mdps: A framework for temporal abstraction in reinforcement learning. *Artificial intelligence*, 112(1-2): 181–211, 1999.
- Teh, Y., Bapst, V., Czarnecki, W. M., Quan, J., Kirkpatrick, J., Hadsell, R., Heess, N., and Pascanu, R. Distral: Robust multitask reinforcement learning. In *Advances in Neural Information Processing Systems*, pp. 4496–4506, 2017.
- Tiomkin, S. and Tishby, N. A unified bellman equation for causal information and value in markov decision processes. *arXiv preprint arXiv:1703.01585*, 2017.
- Tishby, N. and Polani, D. Information theory of decisions and actions. *Perception-Action Cycle*, pp. 601–636, 2011.
- Todorov, E. Linearly-solvable markov decision problems. In *Advances in Neural Information Processing Systems*, 2007.
- Toussaint, M. Robot trajectory optimization using approximate inference. In *Proceedings of the 26th annual international conference on machine learning*, pp. 1049–1056. ACM, 2009.
- Vezhnevets, A. S., Osindero, S., Schaul, T., Heess, N., Jaderberg, M., Silver, D., and Kavukcuoglu, K. Feudal networks for hierarchical reinforcement learning. In *International Conference on Machine Learning*, pp. 3540–3549, 2017.
- Wang, Z., Bapst, V., Heess, N., Mnih, V., Munos, R., Kavukcuoglu, K., and de Freitas, N. Sample efficient actor-critic with experience replay. In *International Conference on Learning Representations*, 2017.
- Xie, S., Galashov, A., Liu, S., Hou, S., Pascanu, R., Heess, N., and Teh, Y. W. Transferring task goals via hierarchical reinforcement learning, 2018. URL <https://openreview.net/forum?id=S1Y6TtJvG>.
- Zhu, H., Gupta, A., Rajeswaran, A., Levine, S., and Kumar, V. Dexterous manipulation with deep reinforcement learning: Efficient, general, and low-cost. *arXiv preprint arXiv:1810.06045*, 2018.
- Ziebart, B. D. *Modeling Purposeful Adaptive Behavior with the Principle of Maximum Causal Entropy*. PhD thesis, Carnegie Mellon University, 2010.
- Zoph, B. and Le, Q. V. Neural architecture search with reinforcement learning. In *International Conference on Learning Representations*, 2017.



## Appendix

### A. A general framework for RL as probabilistic modelling

In Sections 2 and 3 of the main text we have introduced the KL-regularized objective and explored a particular formulation that uses latent variables in the default policy and policy (Section 3 and experiments). The particular choice in Section 3 arises as a special case of a more general framework which we here outline briefly.

For both the default policy and for agent policy we can consider general directed latent variable models of the following form

$$\pi_0(\tau) = \int \pi_0(\tau|y)\pi_0(y)dy, \quad (11)$$

$$\pi(\tau) = \int \pi(\tau|z)\pi(z)dz \quad (12)$$

where both  $y$  and  $z$  can be time varying, e.g.  $y = (y_1, \dots, y_T)$ , and can be causally dependent on the trajectory prefix  $x_t$ , e.g.  $y_t \sim p(\cdot|x_t)$  (and equivalently for  $z$ ). The latent variables can further be continuous or discrete, and  $y_t$  or  $z_t$  can exhibit further structure (and thus include e.g. binary variables that model option termination). The general form of the objective presented in the main text

$$\mathcal{L}(\pi, \pi_0) = \mathbb{E}_\tau \left[ \sum_{t \geq 1} \gamma^t r(s_t, a_t) - \alpha \gamma^t \text{KL}(a_t|x_t) \right],$$

remains valid regardless of the particular form of  $\pi_0$  and  $\pi$ . This form can be convenient when  $\pi_0(a_t|x_t)$  and  $\pi(a_t|x_t)$  are tractable (e.g. when  $z$  or  $y$  have a small number of discrete states or decompose conveniently over time, e.g. as in Fox et al. 2017; Krishnan et al. 2017).

In general, however, latent variables in  $\pi_0$  and  $\pi$  may introduce the need for additional approximations. In this case different models and algorithms can be instantiated based on a) the particular approximation chosen there, as well as b) choices for sharing of components between  $\pi_0$  and  $\pi$ . A possible starting point when  $\pi_0$  contains latent variables is the following lower bound to  $\mathcal{L}$ :

$$\mathcal{L} = \mathbb{E}_\pi [\sum_t r(s_t, a_t)] - \text{KL}[\pi(\tau)||\pi_0(\tau)] \quad (13)$$

$$\geq \mathbb{E}_\pi \left[ \sum_t r(s_t, a_t) + \mathbb{E}_f \left[ \log \frac{\pi_0(\tau, y)}{f(y|\tau)} \right] \right] + \text{H}[\pi(\tau)] \quad (14)$$

$$= \mathbb{E}_\pi \left[ \sum_t r(s_t, a_t) + \mathbb{E}_f [\log \pi_0(\tau|y)] - \text{KL}[f(y|\tau)||\pi_0(y)] + \text{H}[\pi(\tau)] \right]. \quad (15)$$

If  $y_t$  are discrete and take on a small number of values we can compute  $f(y|\tau)$  exactly (e.g. using the forward-backward algorithm as in Fox et al. 2017; Krishnan et al.

2017); in other cases we can learn a parameterized approximation to the true posterior or can conceivably apply mixed inference schemes (e.g. Johnson et al., 2016).

Latent variables in the policy  $\pi$  can require an alternative approximation discussed e.g. in Hausman et al. (2018):

$$\mathcal{L} \geq \mathbb{E}_\pi [\sum_t r(s_t, a_t) + \log \pi_0(\tau) + \log g(z|\tau) + \text{H}[\pi(\tau|z)] + \text{H}[g(Z)]], \quad (16)$$

where  $g$  is a learned approximation to the true posterior  $\pi(z|\tau)$ . This formulation bears interesting similarities with diversity inducing regularization schemes based on mutual information (e.g. Gregor et al., 2017; Florensa et al., 2017) but arises here as an approximation to trajectory entropy. This formulation also has interesting connections to auxiliary variable formulations in the approximate inference literature (Salimans et al., 2014; Agakov & Barber, 2004).

When both  $\pi_0$  and  $\pi$  contain latent variables eqs. (15,16) can be combined. The model described in Section 3 in the main text then arises when the latent variable is “shared” between  $\pi_0$  and  $\pi$  and we effectively use the policy itself as the inference network for  $\pi_0$ :  $f(y|\tau) = \prod_t \pi(y_t|x_t)$ . In this case the objective simplifies to

$$\mathcal{L} \geq \mathbb{E}_\pi \left[ \sum_t r(s_t, a_t) + \log \frac{\pi_0(\tau|z)\pi_0(z)}{\pi(\tau|z)\pi(z)} \right]. \quad (17)$$

When we further set  $\pi_0(\tau|z) = \pi(\tau|z)$  we recover the model discussed in the main text of the paper.

As a proof-of-concept for a model without a shared latent space, with latent variables in  $\pi_0$  but not  $\pi$ , we consider a simple humanoid with 28 degrees of freedom and 21 actuators and consider two different tasks: 1) a dense-reward walking task, in which the agent has to move forward, backward, left, or right at a fixed speed. The direction is randomly sampled at the beginning of an episode and changed to a different direction half-way through the episode and 2) a sparse reward go-to-target task, in which the agent has to move to a target whose location is supplied to the agent as a feature vector similar to those considered in (Galashov et al., 2019).

Figure 11 shows some exploratory results. In a first experiment we compare different prior architectures on the directional walking task. We let the prior marginalize over task condition. We include a feed-forward network, an LSTM, and a latent variable model with one latent variable per time step in the comparison. For the latent variable

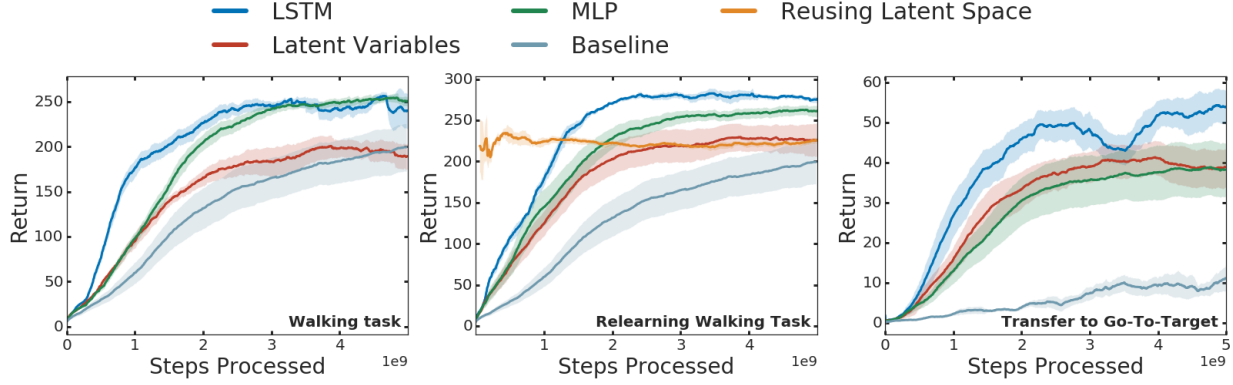


Figure 11. **Results with a latent variable prior.** **Left:** Walking task with the simple humanoid **Center:** Relearning the walking task with fixed priors. **Right:** Transfer to a go-to-target task.

model we chose an inference network  $f(z_t|z_{t-1}, \tau)$  so that eq. (15) decomposes over time. All priors studied in this comparison gave a modest speed-up in learning. While the latent variable prior works well, it does not work as well as the LSTM and MLP priors in this setup. In a first set of transfer experiments, we used the learned priors to learn the walking task again. Again, the learned priors led to a modest speed-up relative to learning from scratch.

We also experimented with parameter sharing for transfer as in the main text. We can freeze the conditional distribution  $\pi_0(a|s, z)$  and learn a new policy  $\pi(z|s)$ , effectively using the learned latent space as an action space. In a second set of experiments, we study how well a prior learned on the walking task can transfer to the sparse go-to-target task. Here all learned priors led to a significant speed up relative to learning from scratch. Small return differences aside, all three different priors considered here solved the task with clear goal directed movements. On the other hand, the baseline only learned to go to very close-by targets. Reusing the latent space did not work well on this task. We speculate that the required turns are not easy to represent in the latent space resulting from the walking task.

## B. Algorithm

This section provides more details about the learning algorithm we use to optimize eq. (9) in the main text. We use different learning algorithms based on the environments. Specifically, we employ SVG(0) (Heess et al., 2015) with experience replay in continuous control environments, and employ IMPALA (Espeholt et al., 2018) in discrete action space environments. Overall, we adapt the base algorithms to support learning hierarchical policy and prior. Unless otherwise mentioned, we follow notations from the main paper.

### B.1. Reparameterized latent for hierarchical policy

To optimize the hierarchical policy, we follow a strategy similar to Heess et al. (2016) and reparameterize  $z_t \sim \pi^H(z_t|x_t)$  as  $z_t = f^H(x_t, \epsilon_t)$ , where  $\epsilon_t \sim \rho(\epsilon_t)$  is a fixed distribution. The  $f^H(\cdot)$  is a deterministic function that outputs distribution parameters. In practice this means that the hierarchical policy can be treated as a flat policy  $\pi(a_t|\epsilon_t, x_t) = \pi^L(a_t|f^H(x_t, \epsilon_t), x_t)$ . We exploit the reparameterized flat policy to employ existing distributed learning algorithm with minimal modification.

### B.2. Continuous control

In continuous control experiments, we employ distributed version of SVG(0) (Heess et al., 2015) augmented with experience replay and off-policy correction algorithm called Retrace (Munos et al., 2016). In the distributed setup, behaviour policies in multiple actors are used to collect off-policy trajectories and a single learner is used to optimize model parameters. The SVG(0) reparameterize a policy  $p(a|s)$  and optimize it by backpropagating gradient from a learned action value function  $Q(a, s)$  through a sampled action  $a$ .

To employ this algorithm, we reparameterize action from flat policy  $a_t \sim \pi_\theta(a_t|\epsilon_t, x_t)$  with parameter  $\theta$  as  $a_t = h_\theta(\epsilon_t, x_t, \xi_t)$ , where  $\xi_t \sim \rho(\xi_t)$  is a fixed distribution, and  $h_\theta(\epsilon_t, x_t, \xi_t)$  is a deterministic function outputting a sample from the distribution  $\pi_\theta(a_t|\epsilon_t, x_t)$ . We also introduce the action value function  $Q(a_t, z_t, x_t)$ . Unlike policies without hierarchy, we estimate the action value depending on the sampled action  $z_t$  as well, so that it could capture the future returns depending on  $z_t$ . Given the flat policy and the action value function, SVG(0) (Heess et al., 2015) suggests to use

following gradient estimate

$$\begin{aligned} & \nabla_{\theta} \mathbb{E}_{\pi_{\theta}(a|\epsilon_t, x_t)} Q(a, z_t, x_t) \\ &= \nabla_{\theta} \mathbb{E}_{\rho(\xi)} Q(h_{\theta}(\epsilon_t, x_t, \xi), z_t, x_t) \\ &= \mathbb{E}_{\rho(\xi)} \frac{\partial Q}{\partial h} \frac{\partial h}{\partial \theta} \approx \frac{1}{M} \sum_{i=1}^M \frac{\partial Q}{\partial h} \frac{\partial h}{\partial \theta} \Big|_{\xi=\xi_i}, \end{aligned} \quad (18)$$

which facilitates using backpropagation. Note that policy parameter  $\theta$  could be learned through  $z_t$  as well, but we decide not to because it tends to make learning unstable.

To learn action value function  $Q(a_t, z_t, x_t)$  and learn policy, we use off-policy trajectories from experience replay. We use Retrace (Munos et al., 2016) to estimate the action values from off-policy trajectories. The main idea behind Retrace is to use importance weighting to correct for the difference between the behavior policy  $\mu$  and the online policy  $\pi$ , while cutting the importance weights to reduce variance. Specifically, we estimate corrected action value with

$$\hat{Q}_t^R = Q_t + \sum_{s \geq t} \gamma^{s-t'} \left( \prod_{i=s}^t c_i \right) \delta_s Q, \quad (19)$$

where  $\delta_s Q = r_s + \gamma(\hat{V}_{s+1} - \alpha \text{KL}_{s+1}) - Q_s$  and  $Q_t = Q(a_t, z_t, x_t)$ .  $\hat{V}_s = \mathbb{E}_{\pi(a|\epsilon_t, x_t)} [Q(a, z_t, x_t)]$  is estimated bootstrap value,  $\text{KL}_s = \text{KL}[\pi^H(z|x_s) \parallel \pi_0^H(z|x_s)] + \text{KL}[\pi^L(a|z_s, x_s) \parallel \pi_0^L(a|z_s, x_s)]$  and  $\gamma$  is discount.  $c_i = \lambda \min \left( \frac{\pi(a_i|\epsilon_i, x_i)}{\mu(a_i|x_i)} \right)$  is truncated importance weight called *traces*.

There are, however, a few notable details that we adapt for our method. Firstly, we do not use the latent  $z_t$  sampled from behaviour policies in actors. This is possible because the latent does not affect the environment directly. Instead, we consider the behavior policy as  $\mu(a|x)$ , which does not depend on latents. This approach is useful since we do not need to consider the importance weight with respect to the HL policy, which might introduce additional variance in the estimator. Another detail is that the KL term at step  $s$  is not considered in  $\delta_s Q$  because the KL at step  $s$  is not the result of action  $a_s$ . Instead, we introduce close form KL at step  $s$  as a loss to compensate for this. The pseudocode for the resulting algorithm is illustrated in Algorithm 2.

### B.3. Discrete action space

For discrete control problems, we use distributed learning with V-trace (Espeholt et al., 2018) off-policy correction. Similarly to the distributed learning setup in continuous control, behaviours policies in multiple actors are used to collect trajectories and a single learner is used to optimize model parameters. The learning algorithm is almost identical to (Espeholt et al., 2018), but there are details that need to be considered mainly because of hierarchy with stochas-

tic latent variable and temporal abstraction. Using negative KL as reward introduces another complication as well.

We consider optimizing objective with infrequent latent

$$\begin{aligned} & \mathcal{L}(\pi, \pi_0) \\ & \geq \mathbb{E}_{\tau} \left[ \sum_{t \geq 1} \gamma^t r(s_t, a_t) - \alpha \gamma^t \mathbb{1}_p(t) \text{KL}(z_t|x_t) \right], \end{aligned} \quad (20)$$

where  $\mathbb{1}_p(t)$  is the indicator function whose value is 1 if  $t \bmod p \equiv 1$  with period  $p$ . This lower bound will be discussed later in Appendix C.2. This infrequent latent case is used for discrete action space experiment, by defining period  $p$  to be equal to the effective step size of the body.

We learn latent conditional value function  $V_{\psi}(z_t, x_t)$  and reparameterized flat policy  $\pi_{\theta}(a_t|\epsilon_t, x_t)$ . V-trace target is computed as follows

$$v_s = V_{\psi}^s + \sum_{t \geq s} \gamma^{t-s} \left( \prod_{i=s}^{t-1} c_i \right) \delta_t V, \quad (21)$$

where  $\delta_t V = \rho_t(r_t + \gamma(V_{\psi}^{t+1} - \text{KL}_{t+1}^p) - V_{\psi}^t)$ ,  $\text{KL}_t^p = \mathbb{1}_p(t) \text{KL}[\pi_{\theta}^H(z|x_t) \parallel \pi_{0,\phi}^h(z|x_t)]$ , and  $V_{\psi}^t := V_{\psi}(z_t, x_t)$  is bootstrapped value at time step  $t$ . Importance weights are computed by  $c_i := \min(\bar{c}, w_i)$  and  $\rho_i := \min(\bar{\rho}, w_i)$ , where  $w_i = \frac{\pi_{\theta}(a_i|\epsilon_i, x_i)}{\mu(a_i|x_i)}$ .  $\bar{c}$  and  $\bar{\rho}$  are truncation coefficient identical to ones from original V-trace paper (Espeholt et al., 2018). Note that here we ignore latent sampled by behaviour policy and just consider states and actions from the trajectory. As discussed in Appendix B.2, we sample latent on-policy and this helps avoiding additional variance introduced with importance weight for HL policy.

Computed V-trace target is used for training both policy and value function with actor-critic algorithm. For training policy, we use policy gradient defined as

$$\sum_{t \geq 1} \rho_t \nabla_{\theta} \log \pi_{\theta}(a_t|z_t, x_t) \delta_t v \quad (22)$$

where  $\delta_t v = \hat{r}_t + \gamma(v_{t+1} - \text{KL}_{t+1}^p) - V_{\psi}^t$  and  $V_{\psi}^t = V_{\psi}(z_t, x_t)$ . We optimize negative KL for time step  $t$  by adding an analytic loss function for HL policy  $\pi_{\theta}^H(z|x_t)$  and default policy  $\pi_{\phi}^H(z|x_t)$

$$\sum_{t \geq 1} \nabla_{\theta, \phi} \mathbb{1}_p(t) \text{KL}[\pi_{\theta}^H(z|x_t) \parallel \pi_{0,\phi}^H(z|x_t)] \quad (23)$$

For training value function, perform gradient descent over  $l_2$  loss

$$\sum_{t \geq 1} (v_t - V_{\psi}^t) \nabla_{\psi} V_{\psi}(z_t, x_t). \quad (24)$$

Additionally we include an action entropy bonus to encourage exploration (Mnih et al., 2016)

$$\sum_{t \geq 1} \nabla_{\theta} H[\pi_{\theta}(a|\epsilon_t, x_t)], \quad (25)$$

where  $H[\cdot]$  is close form entropy. We optimize the gradients from all four objectives jointly. Unlike continuous control, we do not maintain target parameters separately for the discrete action space experiments.

**Algorithm 2** SVG(0) (Heess et al., 2015) with experience replay for hierarchical policy

---

Flat policy:  $\pi_\theta(a_t|\epsilon_t, x_t)$  with parameter  $\theta$   
 HL policy:  $\pi_\theta^H(z_t|x_t)$ , where latent is sampled by reparameterization  $z_t = f_\theta^H(x_t, \epsilon_t)$   
 Default policies:  $\pi_{0,\phi}^H(z_t|x_t)$  and  $\pi_{0,\phi}^L(a_t|z_t, x_t)$  with parameter  $\phi$   
 Q-function:  $Q_\psi(a_t, z_t, x_t)$  with parameter  $\psi$   
 Initialize target parameters  $\theta' \leftarrow \theta, \quad \phi' \leftarrow \phi, \quad \psi' \leftarrow \psi$ .  
 Target update counter:  $c \leftarrow 0$   
 Target update period:  $P$   
 Replay buffer:  $\mathcal{B}$   
**repeat**  
   **for**  $t = 0, K, 2K, \dots T$  **do**  
     Sample partial trajectory  $\tau_{t:t+K}$  with action log likelihood  $l_{t:t+K}$  from replay buffer  $\mathcal{B}$ :  
        $\tau_{t:t+K} = (s_t, a_t, r_t, \dots, r_{t+K}), \quad l_{t:t+K} = (l_t, \dots, l_{t+K}) = (\log \mu(a_t|x_t), \dots, \log \mu(a_{t+K}|x_{t+K}))$   
     Sample latent:  $\epsilon_{t'} \sim \rho(\epsilon), \quad z_{t'} = f_\theta^H(x_{t'}, \epsilon_{t'})$   
     Compute KL:  $\widehat{\text{KL}}_{t'} = \text{KL} \left[ \pi_\theta^H(z|x_{t'}) \parallel \pi_{0,\phi'}^H(z|x_{t'}) \right] + \text{KL} \left[ \pi_\theta^L(a|z_{t'}, x_{t'}) \parallel \pi_{0,\phi'}^L(a|z_{t'}, x_{t'}) \right]$   
     Compute KL for Distillation:  $\widehat{\text{KL}}_{t'}^{\mathcal{D}} = \text{KL} \left[ \pi_\theta^H(z|x_{t'}) \parallel \pi_{0,\phi}^H(z|x_{t'}) \right] + \text{KL} \left[ \pi_\theta^L(a|z_{t'}, x_{t'}) \parallel \pi_{0,\phi}^L(a|z_{t'}, x_{t'}) \right]$   
     Compute action entropy:  $\widehat{\text{H}}_{t'} = \mathbb{E}_{\pi_\theta(a|\epsilon_{t'}, x_{t'})} [\log \pi_\theta(a|\epsilon_{t'}, x_{t'})]$   
     Estimate bootstrap value:  $\widehat{V}_{t'} = \mathbb{E}_{\pi_\theta(a|\epsilon_{t'}, x_{t'})} [Q_{\psi'}(a, z_{t+K}, x_{t+K})] - \alpha \widehat{\text{KL}}_{t+K}$   
     Estimate traces (Munos et al., 2016):  $\hat{c}_{t'} = \lambda \min \left( \frac{\pi_\theta(a_{t'}|\epsilon_{t'}, x_{t'})}{l_{t'}} \right)$   
     Apply Retrace to estimate Q targets (Munos et al., 2016):  
        $\hat{Q}_{t'}^R = Q_{\psi'}(a_{t'}, z_{t'}, x_{t'}) + \sum_{s \geq t'} \gamma^{s-t'} \left( \prod_{i=s}^{t'} \hat{c}_i \right) \left( r_s + \gamma \left( \widehat{V}_{s+1} - \alpha \widehat{\text{KL}}_{s+1} \right) - Q_{\psi'}(a_s, z_s, x_s) \right)$   
     Policy loss:  $\hat{L}_\pi = \sum_{i=t}^{t+K-1} \mathbb{E}_{\pi_\theta(a|\epsilon_i, x_i)} Q_{\psi'}(a, z_i, x_i) - \alpha \widehat{\text{KL}}_i + \alpha_H \widehat{\text{H}}_i$   
     Q-value loss:  $\hat{L}_Q = \sum_{i=t}^{t+K-1} \|\hat{Q}_i^R - Q_\psi(a, z_i, x_i)\|^2$   
     Default policy loss:  $\hat{L}_{\pi_0^H} = \sum_{i=t}^{t+K-1} \widehat{\text{KL}}_i^{\mathcal{D}}$   
      $\theta \leftarrow \theta + \beta_\pi \nabla_\theta \hat{L}_\pi \quad \phi \leftarrow \phi + \beta_{\pi_0^H} \nabla_\phi \hat{L}_{\pi_0^H}$   
      $\psi \leftarrow \psi - \beta_Q \nabla_\psi \hat{L}_Q$   
     Increment counter  $c \leftarrow c + 1$   
     **if**  $c > P$  **then**  
       Update target parameters  $\theta' \leftarrow \theta, \quad \phi' \leftarrow \phi, \quad \psi' \leftarrow \psi$   
        $c \leftarrow 0$   
     **end if**  
**end for**  
**until**

---

**C. Derivations**

This section includes derivations not described in the main paper.

**C.1. Upper bound of KL divergence**

The upper bound of KL divergence in eq. (6) of the main paper is derived as

$$\begin{aligned}
 \text{KL}(a_t|x_t) &\leq \text{KL}(a_t|x_t) + \mathbb{E}_{\pi(a_t|x_t)} [\text{KL}(z_t|a_t, x_t)] \\
 &= \mathbb{E}_{\pi(a_t|x_t)} \left[ \log \frac{\pi(a_t|x_t)}{\pi_0(a_t|x_t)} \right] \\
 &\quad + \mathbb{E}_{\pi(a_t|x_t)} \left[ \mathbb{E}_{\pi(z_t|a_t, x_t)} \left[ \log \frac{\pi(z_t|a_t, x_t)}{\pi_0(z_t|a_t, x_t)} \right] \right] \\
 &= \mathbb{E}_{\pi(a_t, z_t|x_t)} \left[ \log \frac{\pi(a_t, z_t|x_t)}{\pi_0(a_t, z_t|x_t)} \right] = \text{KL}(z_t, a_t|x_t) \\
 &= \mathbb{E}_{\pi(z_t|x_t)} \left[ \log \frac{\pi(z_t|x_t)}{\pi_0(z_t|x_t)} \right] \\
 &\quad + \mathbb{E}_{\pi(z_t|x_t)} \left[ \mathbb{E}_{\pi(a_t|z_t, x_t)} \left[ \log \frac{\pi(a_t|z_t, x_t)}{\pi_0(a_t|z_t, x_t)} \right] \right] \\
 &= \text{KL}(z_t|x_t) + \mathbb{E}_{\pi(z_t|x_t)} [\text{KL}(a_t|z_t, x_t)] \quad (26)
 \end{aligned}$$



with the last expression being tractably approximated using Monte Carlo sampling. Note that:

$$\begin{aligned}\text{KL}(z_t|x_t) &= \text{KL}(\pi^H(z_t|x_t) \parallel \pi_0^H(z_t|x_t)) \\ \text{KL}(a_t|z_t, x_t) &= \text{KL}(\pi^L(a_t|z_t, x_t) \parallel \pi_0^L(a_t|z_t, x_t))\end{aligned}$$

## C.2. Trajectory based derivation of lower bound

This section derives lower bound of eq. (1) in the main paper. We consider high level policy and default policy, whose latent are sampled every  $p$  steps. As in the lower bound in eq. (9) of the main paper, we consider a case where a latent is shared between the policy and the prior. We derive lower bound in trajectory level while considering both the period of high level action  $p$  and the discount  $\gamma$ . Here we introduce notation for trajectory including latent  $\eta = (s_1, z_1, a_1, \dots)$ , not including latent  $\tau = (s_1, a_1, \dots)$ , and including only the sequence of latent  $\zeta = (z_1, z_{1+p}, \dots)$ . In this section, we derive the following lower bound

$$\begin{aligned}\mathcal{L}(\pi, \pi_0) &= \mathbb{E}_\tau \left[ \sum_{t \geq 1} \gamma^t r(s_t, a_t) - \alpha \gamma^t \text{KL}(a_t|x_t) \right] \\ &\geq \mathbb{E}_\eta \left[ \sum_{t \geq 1} \gamma^t r(s_t, a_t) - \alpha \gamma^t \mathbb{1}_p(t) \text{KL}(z_t|x_t) \right. \\ &\quad \left. - \alpha \gamma^t \text{KL}(a_t|z_{p(t)}, x_t) \right],\end{aligned}\tag{27}$$

where  $\mathbb{E}_\tau[\cdot]$  is taken with respect to the distribution over trajectories defined by the agent policy and system dynamics:  $p(s_1) \prod_{t \geq 1} \pi(a_t|x_t) p(s_{t+1}|s_t, a_t)$ .  $\mathbb{E}_\eta[\cdot]$  is taken with respect to the distribution over trajectories of hierarchical policy including latent:  $p(s_1) \prod_{t \geq 1} \pi(a_t|z_{p(t)}, x_t) \pi(z_t|x_t) \mathbb{1}_p(t) p(s_{t+1}|s_t, a_t)$ .  $z_{p(t)}$  is the latest latent sample before time step  $t$  based on the period  $p$  and  $\mathbb{1}_p(t)$  is the indicator function whose value is 1 if  $t \bmod p \equiv 1$  with period  $p$ .

Note that these equations are composed of reward maximization and KL regularization term. We could show equality in reward maximization, and derive lower bound with respect to the KL regularization term. Therefore, we will present equality and inequality with respects to these two terms separately.

### C.2.1. EQUALITY IN REWARD MAXIMIZATION

The equality of reward maximization term holds as follows

$$\begin{aligned}\mathbb{E}_{\pi_\tau} \left[ \sum_{t \geq 1} \gamma^t r(s_t, a_t) \right] &= \int_\tau \pi(\tau) \left[ \sum_{t \geq 1} \gamma^t r(s_t, a_t) \right] d\tau \\ &= \int_\tau \int_\xi \pi(\eta) d\xi \left[ \sum_{t \geq 1} \gamma^t r(s_t, a_t) \right] d\tau \\ &= \int_\tau \int_\xi \pi(\eta) \left[ \sum_{t \geq 1} \gamma^t r(s_t, a_t) \right] d\xi d\tau \\ &= \int_\eta \pi(\eta) \left[ \sum_{t \geq 1} \gamma^t r(s_t, a_t) \right] d\eta \\ &= \mathbb{E}_{\pi_\eta} \left[ \sum_{t \geq 1} \gamma^t r(s_t, a_t) \right].\end{aligned}\tag{28}$$

### C.2.2. LOWER BOUND OF KL REGULARIZATION ON TRAJECTORY

We can show inequality in eq. (27) by deriving it from KL regularization term. We first derive lower bound of trajectory level KL regularization without considering discount.

$$\begin{aligned}\int_\tau \pi(\tau) \log \frac{\pi_0(\tau)}{\pi(\tau)} d\tau &= \int_\tau \pi(\tau) \left[ \log \int_\xi \frac{\pi_0(\tau, \xi)}{\pi(\tau)} d\xi \right] d\tau \\ &= \int_\tau \pi(\tau) \left[ \log \int_\xi \pi(\xi|\tau) \frac{\pi_0(\tau, \xi)}{\pi(\tau)\pi(\xi|\tau)} d\xi \right] d\tau \quad (29) \\ &\geq \int_\tau \pi(\tau) \left[ \int_\xi \pi(\xi|\tau) \log \frac{\pi_0(\tau, \xi)}{\pi(\tau)\pi(\xi|\tau)} d\xi \right] d\tau \\ &= \int_\eta \pi(\eta) \log \frac{\pi_0(\eta)}{\pi(\eta)} d\eta,\end{aligned}$$

where the inequality holds by Jensen's inequality.

### C.2.3. LOWER BOUND OF KL REGULARIZATION WITH DISCOUNT

To derive lower bound with discount, we first introduce the following equation to handle discount in the derivation.

$$\begin{aligned}\sum_{t \geq 1}^T \gamma^t a_t &= \sum_{t \geq 1}^{T-1} \left[ (1-\gamma) \gamma^t \sum_{u \geq 1}^t a_u \right] + \gamma^T \sum_{t \geq 1}^T a_t.\end{aligned}\tag{30}$$

This equality is useful to derive lower bound from summation without discounting ( $\sum_{u \geq 1}^t a_u$ ) and then recombine it with the discounting terms.

To derive lower bound with respect to KL regularization with discount, we first rewrite KL regularization term as a trajectory based KL term. As  $\alpha$  is a constant we will ignore it in the derivation, but it is straightforward to include it. We could turn KL regularization term as a trajectory based KL

$$\begin{aligned}\mathbb{E}_{\pi_\tau} \left[ \sum_{t \geq 1}^T -\text{KL}(a_t|x_t) \right] &= - \int_\tau \pi(\tau) \left[ \sum_{t \geq 1}^T \text{KL}(a_t|x_t) \right] d\tau \\ &= \int_\tau \pi(\tau) \left[ \sum_{t \geq 1}^T \int_{a_t} \pi(a_t|x_t) \log \frac{\pi_0(a_t|x_t)}{\pi(a_t|x_t)} da_t \right] d\tau \\ &= \int_\tau \pi(\tau) \left[ \sum_{t \geq 1}^T \log \frac{\pi_0(a_t|x_t)}{\pi(a_t|x_t)} \right] d\tau \\ &= \int_\tau \pi(\tau) \log \prod_{t \geq 1}^T \frac{\pi_0(a_t|x_t)}{\pi(a_t|x_t)} d\tau \\ &= \int_\tau \pi(\tau) \log \frac{\pi_0(\tau)}{\pi(\tau)} d\tau.\end{aligned}\tag{31}$$

We use eqs. (30) and (31) to rewrite discounted KL regular-

ization as a trajectory based equation.

$$\begin{aligned}
& \mathbb{E}_{\pi_\tau} \left[ \sum_{t \geq 1}^T -\gamma^t \text{KL}(a_t|x_t) \right] \\
&= \mathbb{E}_{\pi_\tau} \left[ -\sum_{t \geq 1}^{T-1} [(1-\gamma)\gamma^t \sum_{u \geq 1}^t \text{KL}(a_u|x_u)] \right. \\
&\quad \left. - \gamma^T \sum_{t \geq 1}^T \text{KL}(a_t|x_t) \right] \\
&= -\sum_{t \geq 1}^{T-1} [(1-\gamma)\gamma^t \mathbb{E}_{\pi_\tau} [\sum_{u \geq 1}^t \text{KL}(a_u|x_u)]] \\
&\quad - \gamma^T \mathbb{E}_{\pi_\tau} [\sum_{t \geq 1}^T \text{KL}(a_t|x_t)] \\
&= \sum_{t \geq 1}^{T-1} [(1-\gamma)\gamma^t \int_{\tau_t} \pi(\tau_t) \log \frac{\pi_0(\tau_t)}{\pi(\tau_t)} d\tau_t] \\
&\quad + \gamma^T \int_{\tau_T} \pi(\tau_T) \log \frac{\pi_0(\tau_T)}{\pi(\tau_T)} d\tau_T,
\end{aligned} \tag{32}$$

where  $\tau_t$  is trajectory until time step  $t$ . We derive lower bound of this trajectory based representation using eq. (29).

$$\begin{aligned}
& \sum_{t \geq 1}^{T-1} [(1-\gamma)\gamma^t \int_{\tau_t} \pi(\tau_t) \log \frac{\pi_0(\tau_t)}{\pi(\tau_t)} d\tau_t] \\
&\quad + \gamma^T \int_{\tau_T} \pi(\tau_T) \log \frac{\pi_0(\tau_T)}{\pi(\tau_T)} d\tau_T \\
&\geq \sum_{t \geq 1}^{T-1} [(1-\gamma)\gamma^t \int_{\eta_t} \pi(\eta_t) \log \frac{\pi_0(\eta_t)}{\pi(\eta_t)} d\eta_t] \\
&\quad + \gamma^T \int_{\eta_T} \pi(\eta_T) \log \frac{\pi_0(\eta_T)}{\pi(\eta_T)} d\eta_T,
\end{aligned} \tag{33}$$

To rearrange this trajectory based representation with KL regularization formulation, we use following equality

$$\begin{aligned}
& \int_{\eta} \pi(\eta) \log \frac{\pi_0(\eta)}{\pi(\eta)} d\eta \\
&= \int_{\eta} \pi(\eta) \log \prod_{t \geq 1}^T \frac{\pi_0(a_t|z_{p(t)}, x_t) \pi_0(z_t|x_t)^{\mathbb{1}_{p(t)}}}{\pi(a_t|z_{p(t)}, x_t) \pi(z_t|x_t)^{\mathbb{1}_{p(t)}}} d\eta \\
&= \int_{\eta} \pi(\eta) \left[ \sum_{t \geq 1}^T \log \frac{\pi_0(a_t|z_{p(t)}, x_t)}{\pi(a_t|z_{p(t)}, x_t)} \right. \\
&\quad \left. + \mathbb{1}_p(t) \log \frac{\pi_0(z_t|x_t)}{\pi(z_t|x_t)} \right] d\eta \\
&= \int_{\eta} \pi(\eta) \left[ \sum_{t \geq 1}^T -\mathbb{1}_p(t) \text{KL}(z_t|x_t) \right. \\
&\quad \left. - \text{KL}(a_t|z_{p(t)}, x_t) \right] d\eta \\
&= \mathbb{E}_{\pi_\eta} \left[ \sum_{t \geq 1}^T -\mathbb{1}_p(t) \text{KL}(z_t|x_t) - \text{KL}(a_t|z_{p(t)}, x_t) \right],
\end{aligned} \tag{34}$$

where  $z_{p(t)}$  is the latest latent sample before time step  $t$  based on the period  $p$ .

We rearrange eq. (33) based on eqs. (30) and (34).

$$\begin{aligned}
& \sum_{t \geq 1}^{T-1} [(1-\gamma)\gamma^t \int_{\eta_t} \pi(\eta_t) \log \frac{\pi_0(\eta_t)}{\pi(\eta_t)} d\eta_t] \\
&\quad + \gamma^T \int_{\eta_T} \pi(\eta_T) \log \frac{\pi_0(\eta_T)}{\pi(\eta_T)} d\eta_T \\
&= -\sum_{t \geq 1}^{T-1} [(1-\gamma)\gamma^t \mathbb{E}_{\pi_\eta} [\sum_{u \geq 1}^t \mathbb{1}_p(u) \text{KL}(z_u|x_u) \\
&\quad + \text{KL}(a_u|z_{p(u)}, x_u)]] \\
&\quad - \gamma^T \mathbb{E}_{\pi_\eta} [\sum_{t \geq 1}^T \mathbb{1}_p(t) \text{KL}(z_t|x_t) \\
&\quad + \text{KL}(a_t|z_{p(t)}, x_t)] \\
&= -\mathbb{E}_{\pi_\eta} [\sum_{t \geq 1}^{T-1} [(1-\gamma)\gamma^t \sum_{u \geq 1}^t \mathbb{1}_p(u) \text{KL}(z_u|x_u) \\
&\quad + \text{KL}(a_u|z_{p(u)}, x_u)] \\
&\quad + \gamma^T \sum_{t \geq 1}^T \mathbb{1}_p(t) \text{KL}(z_t|x_t) + \text{KL}(a_t|z_{p(t)}, x_t)] \\
&= \mathbb{E}_{\pi_\eta} [\sum_{t \geq 1}^T -\mathbb{1}_p(t) \gamma^t \text{KL}(z_t|x_t) - \gamma^t \text{KL}(a_t|z_{p(t)}, x_t)].
\end{aligned} \tag{35}$$

By combining all results, we obtain the following inequality.

$$\begin{aligned}
\mathcal{L}(\pi, \pi_0) &= \mathbb{E}_\tau [\sum_{t \geq 1} \gamma^t r(s_t, a_t) - \alpha \gamma^t \text{KL}(a_t|x_t)] \\
&\geq \mathbb{E}_\eta [\sum_{t \geq 1} \gamma^t r(s_t, a_t) - \alpha \gamma^t \mathbb{1}_p(t) \text{KL}(z_t|x_t) \\
&\quad - \alpha \gamma^t \text{KL}(a_t|z_{p(t)}, x_t)].
\end{aligned} \tag{36}$$

## D. Additional Experimental Results

### D.1. Alternative training regimes

In the main paper, we present results based on learning speed with respect to the number of time steps processed by learner in distributed learning setup. Note that the number of time steps processed by the learner does not necessarily correspond to the number of collected trajectory time steps because of the use of experience replay, which allows to learning to proceed regardless of the amount of collected trajectories. We also experimented with two alternative training regimes to ensure that the speedup results reported are consistent. In Figure 12, we compare the learning curves for our method against the SVG-0 and DISTRAL baselines in a quasi on-policy training regime similar to that of (Espeholt et al., 2018). In Figure 13, we perform a similar comparison in the original replay based off-policy training regime but with a single actor generating the data. In both cases, our method learns faster than both baselines.

### D.2. Information asymmetry in task transfer

Figure 14 illustrates the necessity of information asymmetry and KL regularization during transfer. Here we train the agent on the Move box Or Go to Target task with different information given to the LL and then transfer to Move Box and GTT. Therefore the distributions of the trajectories during training and those required for transfer should be similar.

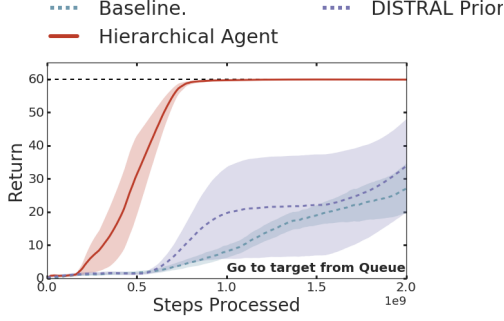


Figure 12. **Learning curves with quasi on-policy training regime.** Go to 1 of 3 targets, Ant. AR-1 process.

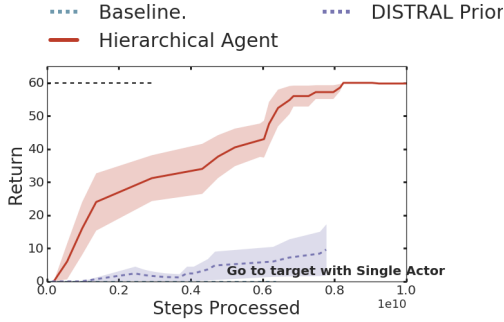


Figure 13. **Learning curves with a single actor.** Go to 1 of 3 targets, Ant. AR-1 process.

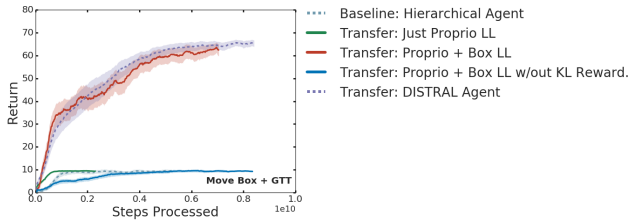


Figure 14. **Analysis on task transfer results.** Transfer from move box or go to target to move box and go to target with Ant and AR-1 process.

As the figure shows, we observe successful transfer only when the box position is given to the LL controller and KL regularization is used during transfer. Failed approaches usually converge to suboptimal policies, where the agent succeeds on the go to target task, but cannot move the box appropriately. In this transfer scenario, giving box position as input to LL controller is one way to specify inductive bias, which turns out to be useful to move box appropriately in target task. Interestingly, the unstructured DISTRAL prior performs comparatively to our method in this experiment. We hypothesize that for tasks that take longer to learn, the benefit of the immediate parameter transfer in our approach is not as strong since this also leads to a fixed lower level behavior that cannot be adapted to the task. In this sense, the DISTRAL baseline is expected to be asymptotically

stronger.

## E. Environments

### E.1. Discrete control

We construct a **discrete go to target** task in 2D grid world. An agent and goal are randomly placed in an  $8 \times 8$  grid and the agent is given a reward of 1.0 for reaching the goal. The episode terminates when the agent reaches the goal or after 400 time steps. Additionally, the agent receives a penalty of -0.1 for every time step and a penalty of -0.2 if it collides with the walls. The body agnostic tasks observation is global x, y coordinate of agent and goal.

We consider a body that moves in any of 4 directions in the grid (up, down, left, right). We define different bodies based on their effective step size. The effective step size is the number of consecutive movements required to make a single displacement in the grid. Specifically, a body has 2 dimensional internal coordinate  $[-n + 1, n - 1]^2$  with effective step size  $n$ . Agent’s action primarily affect the internal coordinate and it brings displacement to the external coordinate only if a value exceed its minimum or maximum. In this case, agent move 1 step in external coordinate and internal coordinate for the corresponding dimension is reset to 0. We denote different bodies with their step size (e.g. 1-step). We assume that the latent  $z_t$  is sampled every  $n$  steps, where  $n$  is the effective step size.

### E.2. Continuous control

In this section, we describe detailed configuration of the continuous control tasks and bodies.

#### E.2.1. TASKS

**Go to 1 of K targets** On a fixed  $8 \times 8$  area, an agent and K targets are randomly placed at the beginning of episodes. In each episode, one of the K targets are randomly selected, and the agent should reach the selected target within 400 time steps. When the agent reach the selected target, the agent receives a reward of 60 and the episode terminates. Egocentric coordinates of K targets and an onehot vector representing one of the K targets are provided as task observations.

**Move box to 1 of K targets** On a fixed  $3 \times 3$  area, an agent, a box and K targets are randomly placed at the beginning of episodes. In each episode, one of the K targets are randomly selected, and the agent should move the box to the selected target within 400 time steps. When the box is placed on the selected target, the agent receives a reward of 60 and the episode terminates. Egocentric coordinates of K targets and 6 corner of the box is provided as task observations with an onehot vector representing one of the K targets.

**Move K boxes to K targets** On a fixed  $3 \times 3$  area, an agent, K boxes and K targets are randomly placed at the beginning of episodes. In each episode, targets of each boxes are randomly assigned, and the agent should move all boxes to each of the corresponding targets within 400 time steps. Whenever a box is placed on the correct target, the agent receives a reward of 10, and the agent receives an additional reward of 50 when every box is placed to corresponding targets correctly. Egocentric coordinates of K targets and 6 corners of boxes are provided as task observations, and K onehot vectors are provided to represent targets for each box.

**Move heavier box** This task is essentially a variation of the move box to 1 of k targets task but with the box weight increased by a factor of 3x. The task can be solved by either changing the actuation signal to push harder and thus move the box to the target quickly or by taking small substeps and inching the box close to the target. Crucially in this task the episode ends in 100 time steps and so one behavior is preferred over another. A sparse reward of 60 is provided to the agent on solving the task.

**Gather boxes** On a fixed  $3 \times 3$  area, an agent and K boxes are randomly locate at the beginning of episodes. In each episode, the agent should gather all the boxes within 400 time steps so that the boxes are contacted to each other. The agent receives a reward of 60 when it successfully gathers boxes. Egocentric coordinates of 6 corners of boxes are provided as task observations.

**Move box or go to target** This task is a combination of the go to 1 of 2 targets task and the move box to 1 of 2 targets task. On each episode one of the two tasks is randomly sampled so that with probability 0.5 the agent must go to one of the 2 targets and with probability 0.5 it must push a box to a specific target. The agent receives a reward of 60 for successfully completing the corresponding task. Egocentric coordinates of both targets as well as the corners of the box are provided as task observations along with an encoding describing the specific task instance.

**Move box and go to target** This task contains the move box to 1 of 2 targets and go to 1 of 2 targets as two sub-tasks. In each episode, the walker must push the box to a target and then go to another target. A reward of 10 is awarded for each sub task that is completed and a bonus reward of 50 is awarded for completing both tasks. Egocentric coordinates of both targets as well as the corners of the box are provided as task observations.

**Go to target from vision** This task is identical to the Go to 1 of K targets, but the task observation is egocentric vision. Instead of egocentric target coordinates, the agent observes a  $64 \times 64$  image captured by the agent’s egocentric camera. The agent needs to recognize visual patterns of the targets and figure out the correct target (always colored

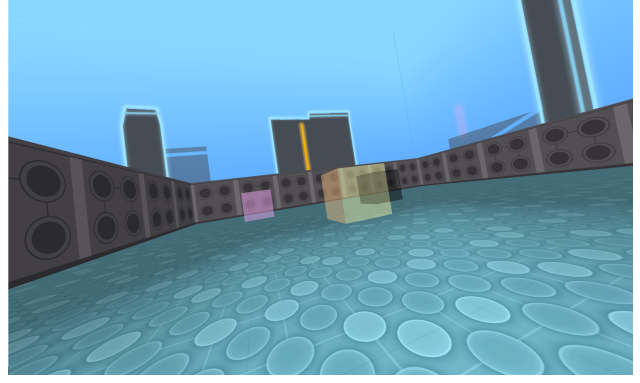


Figure 15. Vision input for Go to target from vision.

Task	Walker	LL information
Go to 1 of K Targets	Ant	Proprioception
Move box to target	Ant	Proprioception + Box
2 Boxes and 2 Targets	Ball	Proprioception + Boxes + Targets
Move Box or Go to Target (I)	Ant	Proprioception
Move Box or Go to Target (II)	Ant	Proprioception + Box
Gather Boxes	Ball	Proprioception + Boxes + Targets

Table 1. Information provided to the lower level controller for each task.

black in this case). Figure 15 illustrates the egocentric visual observation before being rescaled to  $64 \times 64$ .

### E.2.2. BODIES

We use three different bodies: Ball, Ant, and Quadruped. Ball and Ant have been used in several previous works (Heess et al., 2017; Xie et al., 2018; Galashov et al., 2019), and we introduce Quadruped as a more complex variant of the Ant. The **Ball** is a body with 2 actuators for moving forward or backward, turning left, and turning right. The **Ant** is a body with 4 legs and 8 actuators, which moves its legs to walk and to interact with objects. The **Quadruped** is similar to Ant, but with 12 actuators. Each body has different proprioception (proprio) as a body specific observation.

### E.2.3. DETAILS OF INPUT TO THE LOWER LEVEL

1 illustrates the information provided to the lower level for each of the tasks for the speedup and transfer settings considered in the main text. In these cases, the HL received full information. For the tasks where the body was transferred,



the LL was only given proprioceptive information while the HL received all other information relevant to the task.

## F. Experimental Settings

### F.1. General settings

Throughout the experiments, we use 32 actors to collect trajectories and a single learner to optimize the model. We plot average episode return with respect to the number of steps processed by the learner. Note that the number of steps is different from the number of agent’s interaction with environment, because the collected trajectories are processed multiple times by a centralized learner to update model parameters. When learning from scratch we report results as the mean and standard deviation of average returns for 5 random seeds. For the transfer learning experiments, we use 5 seed for the initial training, and then transfer all pretrained models to a new task, and train two new HL or LL controllers (two random seeds) per model on the transfer task. Thus, in total, 10 different runs are used to estimate mean and standard deviations of the average returns. Hyperparameters, including KL cost and action entropy regularization cost, are optimized on a per-task basis. More details are provided in Appendix G.

### F.2. DISTRAL with parameter sharing

We introduced two baselines as variants of DISTRAL prior sharing parameters between the agent policy and the default policy. **DISTRAL prior 2 cols** uses a 2-column architecture (see Teh et al. (2017)), where the default policy network is reused in combination with another network (column) to output the final policy distribution. In this configuration, the default policy network does not access to task information, but another network (column) access to the full information. In **DISTRAL shared prior**, the policy network is reused to output the default policy distribution based on an additional branch on top of it. As default policy is constructed on policy network, information asymmetry is not used in this baseline.

## G. Hyper parameters

Fully connected neural networks are used as function approximators for both the actor and the critic in the agent. In case of tasks with boxes, a separate common single layer MLP was used as a *box encoder torso*. Separate processing networks were implemented for *proprioception* for the baselines. For all tasks, multiple values were swept for actor networks and torso sizes with 5 random seeds each. ELU activations were used throughout. We use separate optimizers and learning rates for the actor and critic networks. For the hierarchical networks, fully connected MLP networks were used for the higher level and lower level policy cores. The

relative contribution of the KL regularization to the reward was controlled by a *posterior entropy cost* which we denote  $\alpha$ .

Below we provide the default hyperparameters used across tasks followed by the best parameters from the baselines and the hierarchical networks for each task.

### G.1. Default parameters

*Actor learning rate,  $\beta_{pi} = 1e-4$ .*

*Critic learning rate,  $\beta_{pi} = 1e-4$ .*

*DISTRAL baseline default policy learning rate,  $\beta_{pi} = 5e-4$ .*

*Target network update period = 100.*

*DISTRAL policy target network update period = 100.*

*Baseline Actor network: MLP with sizes (200, 100).*

*Baseline Critic network: MLP with sizes (400, 300).*

*DISTRAL baseline default policy network: MLP with sizes (200, 100).*

*HL policy network: MLP with sizes (200, 10).*

*LL policy network: MLP with sizes (200, 100).*

*Box encoder network: MLP with sizes (50).*

*Batch size: 512.*

*Unroll length: 10.*

*Entropy bonus,  $\lambda = 1e-4$ .*

*Posterior Entropy cost for HL,  $\alpha = 1e-3$ .*

*Posterior Entropy cost for DISTRAL default policy,  $\alpha = 0.01$*

*Distillation cost for DISTRAL default policy,  $\alpha = 0.01$*

*Number of actors: 32*

### G.2. Per-task parameters

#### Ant: Move Box to Target

*Entropy bonus,  $\lambda = 1e-3$ .*

*Policy network for Gaussian Prior: MLP with sizes (200, 100).*

*Action Entropy cost for Isotropic Gaussian Prior: = 0.*

*Action Entropy cost for AR-1 Prior: = 0.*

*AR Parameter: = 0.9*

*Posterior Entropy cost for AR-1 Prior,  $\alpha = 1e-4$ .*

#### Ant: Go to 1 of 3 Targets

*Action Entropy cost for DISTRAL default policy = 0.*

*AR Parameter:* = 0.95

*Distillation cost for DISTRAL default policy,  $\alpha = 1.0$*

**Ball: 2 Boxes to 2 Targets**

*Distillation cost for DISTRAL default policy,  $\alpha = 0.1$*

*Box encoder network:* MLP with sizes (100, 20).

*HL policy network for AR-Learned Prior:* MLP with sizes (200, 4).

**Ant: Move Box to 1 of 3 Targets**

*AR Parameter for baseline:* = 0.9

*Policy network for AR-1 Transfer Prior:* MLP with sizes (200, 10).

*Policy network for Gaussian Transfer Prior:* MLP with sizes (200, 4).

*Policy network for AR-Learned Transfer Prior:* MLP with sizes (200, 4).

*Posterior Entropy cost for AR-Learned Transfer Prior,  $\alpha = 1e-2$ .*

*Action Entropy cost for AR-Learned Transfer Prior:* =  $1e-4$ .

**Ball: Gather boxes**

*Policy network for Gaussian Transfer Prior:* MLP with sizes (200, 4).

*Policy network for AR-Learned Transfer Prior:* MLP with sizes (200, 4).

*DISTRAL Actor learning rate,  $\beta_{pi} = 5e-4$ .*

*DISTRAL default policy distillation cost* = 0.01.

**Ant: Move Box and Go to Target**

*Policy network for AR-1 Prior:* MLP with sizes (200, 10).

**Ball to Ant: Go to Target**

Unless otherwise specified, for all the body transfer tasks an *action entropy cost* of  $1e-4$  worked best across tasks.

*HL Policy network for agent from scratch:* MLP with sizes (100, 4)

**Ball to Ant: Move Box to Target**

*HL Policy network for agent from scratch:* MLP with sizes (100, 4)

*Posterior entropy cost for transfer agent:*  $1e-5$

**Ant to Quadruped: Move Box to Target**

*Posterior entropy cost for transfer agent:*  $1e-2$

*Action entropy cost for transfer agent:*  $1e-5$

**Ant to Quadruped: Go To Target:**

*HL Policy network for agent from scratch:* MLP with sizes (20)

**Ant to Quadruped: Go To Target From Vision:**

*HL Policy network:* Residual Network with an embedding size of (256,)